Long Chain Branched Polypropylene with Nucleating Agent

Bc. Jitka Kučerová

Master thesis
2009/2010

Tomas Bata University in Zlín
Faculty of Technology

Univerzita Tomáše Bati ve Zlíně
Fakulta technologická
Ústav inženýrství polymerů
akademický rok: 2009/2010

ZADÁNÍ DIPLOMOVÉ PRÁCE

(PROJEKTU, UMĚLECKÉHO DÍLA, UMĚLECKÉHO VÝKONU)

Jméno a příjmení:	**Bc. Jitka KUČEROVÁ**
Studijní program:	**N 2808 Chemie a technologie materiálů**
Studijní obor:	**Inženýrství polymerů**
Téma práce:	**Rozvětvený polypropylen s nukleačním činidlem**

Zásady pro vypracování:

The aim of this Master thesis is to study the crystallization and properties of long chain branched polypropylene (LCB PP) containing commercial α-nucleating/clarifying agent Millad 3988 based on 1,3;2,4-bis(3,4-dimethylbenzylidene)sorbitol. For comparison also standard polypropylene will be studied. LCB PP has been developed to improve melt strength, thus it can be advantageously processed by techniques such as thermoforming of blow moulding. These methods are usually used for packaging application where also clarity is often required. Thus, the understanding of crystallization of LCB PP containing clarifying agent is on high interest. In the work, samples from LCB PP and also standard PP will be compression moulded using several conditions. Than, the structure and properties will be evaluated via several methods such as X-ray scattering, differential scanning calorimetry, optical microscopy, opacity measurement and tensile testing.

Rozsah práce:

Rozsah příloh:

Forma zpracování diplomové práce: **tištěná/elektronická**

Seznam odborné literatury:

1.Karger-Kocsis, J.: Polypropylene - An A-Z Reference, Springer -- Verlag, 1999, ISBN:0-412-80200-7
2.Maier, C.; Calafut, T.: Polypropylene - The Definitive User's Guide and Databook,William Andrew Publishing/Plastics Design Library, 1998, ISBN: 1-884207-58-8
3.Weiqing,W; Weiguo,H:Long Chain Branched Isotactic Polypropylene, Macromolecules, 2002, 35, P:3838-3843
4. Maier, C., Calafut, T., Polypropylene: The definitive user's guide and databook, ISBN 1884207588, 1998, William Andrew Inc. Page 141

Vedoucí diplomové práce: **Ing. Jana Navrátilová, Ph.D.**
Ústav inženýrství polymerů

Datum zadání diplomové práce: **15. února 2010**

Termín odevzdání diplomové práce: **14. května 2010**

Ve Zlíně dne 15. února 2010

doc. Ing. Petr Hlaváček, CSc.
děkan

L.S.

doc. Ing. Roman Čermák, Ph.D.
ředitel ústavu

Příjmení a jméno: Jitka Kučerová Obor: inženýrství polymerů

PROHLÁŠENÍ

Prohlašuji, že

- beru na vědomí, že odevzdáním diplomové/bakalářské práce souhlasím se zveřejněním své práce podle zákona č. 111/1998 Sb. o vysokých školách a o změně a doplnění dalších zákonů (zákon o vysokých školách), ve znění pozdějších právních předpisů, bez ohledu na výsledek obhajoby [1)];
- beru na vědomí, že diplomová/bakalářská práce bude uložena v elektronické podobě v univerzitním informačním systému dostupná k nahlédnutí, že jeden výtisk diplomové/bakalářské práce bude uložen na příslušném ústavu Fakulty technologické UTB ve Zlíně a jeden výtisk bude uložen u vedoucího práce;
- byl/a jsem seznámen/a s tím, že na moji diplomovou/bakalářskou práci se plně vztahuje zákon č. 121/2000 Sb. o právu autorském, o právech souvisejících s právem autorským a o změně některých zákonů (autorský zákon) ve znění pozdějších právních předpisů, zejm. § 35 odst. 3 [2)];
- beru na vědomí, že podle § 60 [3)] odst. 1 autorského zákona má UTB ve Zlíně právo na uzavření licenční smlouvy o užití školního díla v rozsahu § 12 odst. 4 autorského zákona;
- beru na vědomí, že podle § 60 [3)] odst. 2 a 3 mohu užít své dílo – diplomovou/bakalářskou práci nebo poskytnout licenci k jejímu využití jen s předchozím písemným souhlasem Univerzity Tomáše Bati ve Zlíně, která je oprávněna v takovém případě ode mne požadovat přiměřený příspěvek na úhradu nákladů, které byly Univerzitou Tomáše Bati ve Zlíně na vytvoření díla vynaloženy (až do jejich skutečné výše);
- beru na vědomí, že pokud bylo k vypracování diplomové/bakalářské práce využito softwaru poskytnutého Univerzitou Tomáše Bati ve Zlíně nebo jinými subjekty pouze ke studijním a výzkumným účelům (tedy pouze k nekomerčnímu využití), nelze výsledky diplomové/bakalářské práce využít ke komerčním účelům;
- beru na vědomí, že pokud je výstupem diplomové/bakalářské práce jakýkoliv softwarový produkt, považují se za součást práce rovněž i zdrojové kódy, popř. soubory, ze kterých se projekt skládá. Neodevzdání této součásti může být důvodem k neobhájení práce.

Ve Zlíně 18.5.2010

Kučerová Jitka

[1] zákon č. 111/1998 Sb. o vysokých školách a o změně a doplnění dalších zákonů (zákon o vysokých školách), ve znění pozdějších právních předpisů, § 47 Zveřejňování závěrečných prací:
(1) Vysoká škola nevýdělečně zveřejňuje disertační, diplomové, bakalářské a rigorózní práce, u kterých proběhla obhajoba, včetně posudků oponentů a výsledku obhajoby prostřednictvím databáze kvalifikačních prací, kterou spravuje. Způsob zveřejnění stanoví vnitřní předpis vysoké školy.
(2) Disertační, diplomové, bakalářské a rigorózní práce odevzdané uchazečem k obhajobě musí být též nejméně pět pracovních dnů před konáním obhajoby zveřejněny k nahlížení veřejnosti v místě určeném vnitřním předpisem vysoké školy nebo není-li tak určeno, v místě pracoviště vysoké školy, kde se má konat obhajoba práce. Každý si může ze zveřejněné práce pořizovat na své náklady výpisy, opisy nebo rozmnoženiny.
(3) Platí, že odevzdáním práce autor souhlasí se zveřejněním své práce podle tohoto zákona, bez ohledu na výsledek obhajoby.
[2] zákon č. 121/2000 Sb. o právu autorském, o právech souvisejících s právem autorským a o změně některých zákonů (autorský zákon) ve znění pozdějších právních předpisů, § 35 odst. 3:
(3) Do práva autorského také nezasahuje škola nebo školské či vzdělávací zařízení, užije-li nikoli za účelem přímého nebo nepřímého hospodářského nebo obchodního prospěchu k výuce nebo k vlastní potřebě dílo vytvořené žákem nebo studentem ke splnění školních nebo studijních povinností vyplývajících z jeho právního vztahu ke škole nebo školskému či vzdělávacího zařízení (školní dílo).
[3] zákon č. 121/2000 Sb. o právu autorském, o právech souvisejících s právem autorským a o změně některých zákonů (autorský zákon) ve znění pozdějších právních předpisů, § 60 Školní dílo:
(1) Škola nebo školské či vzdělávací zařízení mají za obvyklých podmínek právo na uzavření licenční smlouvy o užití školního díla (§ 35 odst. 3). Odpírá-li autor takového díla udělit svolení bez vážného důvodu, mohou se tyto osoby domáhat nahrazení chybějícího projevu jeho vůle u soudu. Ustanovení § 35 odst. 3 zůstává nedotčeno.
(2) Není-li sjednáno jinak, může autor školního díla své dílo užít či poskytnout jinému licenci, není-li to v rozporu s oprávněnými zájmy školy nebo školského či vzdělávacího zařízení.
(3) Škola nebo školské či vzdělávací zařízení jsou oprávněny požadovat, aby jim autor školního díla z výdělku jím dosaženého v souvislosti s užitím díla či poskytnutím licence podle odstavce 2 přiměřeně přispěl na úhradu nákladů, které na vytvoření díla vynaložily, a to podle okolností až do jejich skutečné výše; přitom se přihlédne k výši výdělku dosaženého školou nebo školským či vzdělávacím zařízením z užití školního díla podle odstavce 1.

ABSTRAKT

Cílem této diplomové práce je studie krystalizace a vlastností polypropylenu s dlouhými větvemi (LCB PP), který obsahuje komerčně dostupné α-nukleační/zjasňující činidlo Millad 3988 na bázi 1,3;2,4-bis(3,4-dimetylbenzyliden)sorbitolu. Pro srovnání byl studován také standardní polypropylen. LCB PP byl vyvinut pro zlepšení pevnosti taveniny, a tak se může výhodně používat pro zpracování metodami, jako je tvarování či vyfukování. Tyto metody se obvykle používají pro výrobu obalů, kde se často požaduje také průzračnost materiálu. Z toho důvodu je pochopení krystalizace LCB PP obsahující zjasňující činidlo prakticky důležité.

V této práci byly vzorky z LCB PP, a také ze standardního PP zkrystalizovány za použití různých podmínek. Dále pak byla hodnocena kinetika krystalizace a morfologie. Byly také zkoumány optické vlastnosti. Bylo zjištěno, že přidání Milladu 3988 výrazně neovlivňuje krystalizaci a morfologii LCB PP.

Klíčová slova: rozvětvený polypropylen, zjasňující činidlo, Millad 3988, krystalizace

ABSTRACT

The aim of this Master thesis is to study the crystallization and properties of long chain branched polypropylene (LCB PP) containing commercial α-nucleating/clarifying agent Millad 3988 based on 1,3;2,4-bis(3,4-dimethylbenzylidene)sorbitol. For comparison also standard polypropylene is studied. LCB PP has been developed to improve melt strength, thus it can be advantageously processed by techniques such as thermoforming of blow molding. These methods are usually used for packaging application where also clarity is often required. Thus, the understanding of crystallization of LCB PP containing clarifying agent is on high interest.

In the work, samples from LCB PP and also standard PP are crystallized using several conditions. Then the crystallization kinetics and morphology is evaluated. Also optical properties are analyzed. It has been found that the addition of Millad 3899 does not significantly influences the crystallization and morphology of LCB PP.

Keywords: Long chain branched polypropylene, clarifying agent, Millad 3988, crystallization

ACKNOWLEDGEMENTS

I would like to express my deepest gratitude and thanks to the supervisor of my master thesis Jana Navrátilová for her guidance and support. My thanks go to as well to the whole academic and pedagogic board of the Faculty of Technology on Tomas Bata University in Zlin for their education and teaching efforts which made this possible.

CONTENTS

INTRODUCTION

Physical and mechanical properties of polymers are the most important from their application point of view. Isotactic polypropylene (iPP) possesses very good price/performance ratio and thus is widely applied, namely in automotive industry, packaging etc.

Polypropylene (PP) was first produced by Professor Giulio Natta in Spain in 1954. Natta utilized catalysts developed for the polyethylene industry and applied the technology to propylene gas. Commercial production began in 1957 and polypropylene usage has displayed strong growth from this date. The versatility of the polymer (the ability to adapt to a wide range of fabrication methods and applications) has sustained growth rates enabling polypropylene to challenge the market share of a host of alternative materials in plethora of applications. Metallocene based catalysis (since 1980s) enable to obtain polypropylene with required structure like an isotactic, syndiotactic and atactic stereoisomers [1].

Isotactic polypropylene is the most commercially used stereoisomer of PP. It has many desirable and beneficial physical properties such as low density, high melting point and chemical resistance. However, iPP has low melt strength and no strain hardening which limits its use in foaming, thermoforming and so on. The most effective method to improve the melt strength of PP is to introduce long chain branching (LCB) onto the polypropylene backbone.

Several approaches have been developed to make branched polypropylenes. Some include post-reactor treatments such as electron beam irradiation, peroxide curing and grafting; other use in-reactor copolymerization. The branches in irradiated or peroxide treatment polymers are generated thought radical-induce random chain scission followed by recombination. Thus, the products are complex and the processes may be difficult to control [2].

The change of molecular architecture in long chain branched polypropylene (LCB PP) can affect not only rheological property but also crystallization property of PP [3]. However, the crystallization behavior of linear and LCB PP has seldom been studied in detail. Many studies have been focused on the crystallization of grafted iPP. It is widely accepted that grafted iPP partly acts as a nucleating agent for the matrix and accelerates the crystallization rate. It can be concluded from limited literatures [4, 5] that LCB PP has

higher crystallization temperature, shorter crystallization time, and broader melting range when compared with linear PP.

The properties and processing of the polymers are often modified via addition of nucleating agents, especially in the case of polymers with low crystallization rate. This modification is quite common in iPP. Mostly the α-nucleating agents are used not only to speed the crystallization and thus the processing, but also to improve clarity of the material. For this purpose, nucleating/clarifying agents based on sorbitol are often used [6, 7, 8]. The crystallization and mechanical properties of iPP containing α-nucleating/clarifying agents are well documented in the literature [e.g. 9, 10]. However, the behaviour of LCB PP modified by such nucleating agents is not complexly described yet.

Thus, in this work, the crystallization and morphology of LCB PP with commercial sorbitol-based α-nucleating/clarifying agent is investigated. For this purpose, differential scanning calorimetry, wide-angle X-ray scattering and polarized light microscopy were used. Also optical properties were measured.

I. THEORY

1 LONG CHAIN BRANCHED POLYPROPYLENE

Isotactic polypropylene (iPP) has many advantageous properties when compared to other commodity thermoplastics, such as PE, in all its forms, and PVC: it has high melting point and low density; it shows excellent chemical resistance and high tensile modulus. Commercial iPP is produced via Ziegler-Natta or metallocene catalysis; it consists of highly linear chains and has a relatively narrow molecular weight distribution. As a consequence, the iPP has relatively low melt strength and rather poor processing characteristics in processes where the type of flow is predominantly elongation. Such processes are foaming, thermoforming, extrusion coating and blow molding. The most efficient way to enhance the melt strength of polymers with linear chains is by grafting long chain branches (LCB) on them [3].

1.1 Methods of production

Long chain branched polypropylene (LCB PP) is mostly produced by grafting long chain branches on the isotactic polypropylene linear backbone, either by electron beam irradiation or in the melt by using peroxides with relatively low decomposition temperature. These methods produce LCB PP with broadened molecular weight distribution and complex branch structures. There are also some reports on the direct synthesis of long chain branched polypropylene: using metallocene catalysis either directly or via the addition of pre-made iPP macromonomers; using conjugated diene monomers; via the metallocene-mediated polymerization of polypropylene in the presence of T-reagent p-(3-butenyl)styrene. Another conceivable method is the modification by peroxide reactions in the solid state in the presence or not of a co-agent [11].

1.1.1 Solid state reactions with co-agent

Co-agents can be used in combination with the organic peroxide to produce LCB on iPP. It can be divinylbenzene (DVB), furfuryl sulphide (FS) or 1,4-benzenediol (RES). The co-agents are bifunctional monomers, which are able, using their multiple function groups, to react with macro-radicals formed on the neighboring iPP chains and form chemical bridges between them [11].

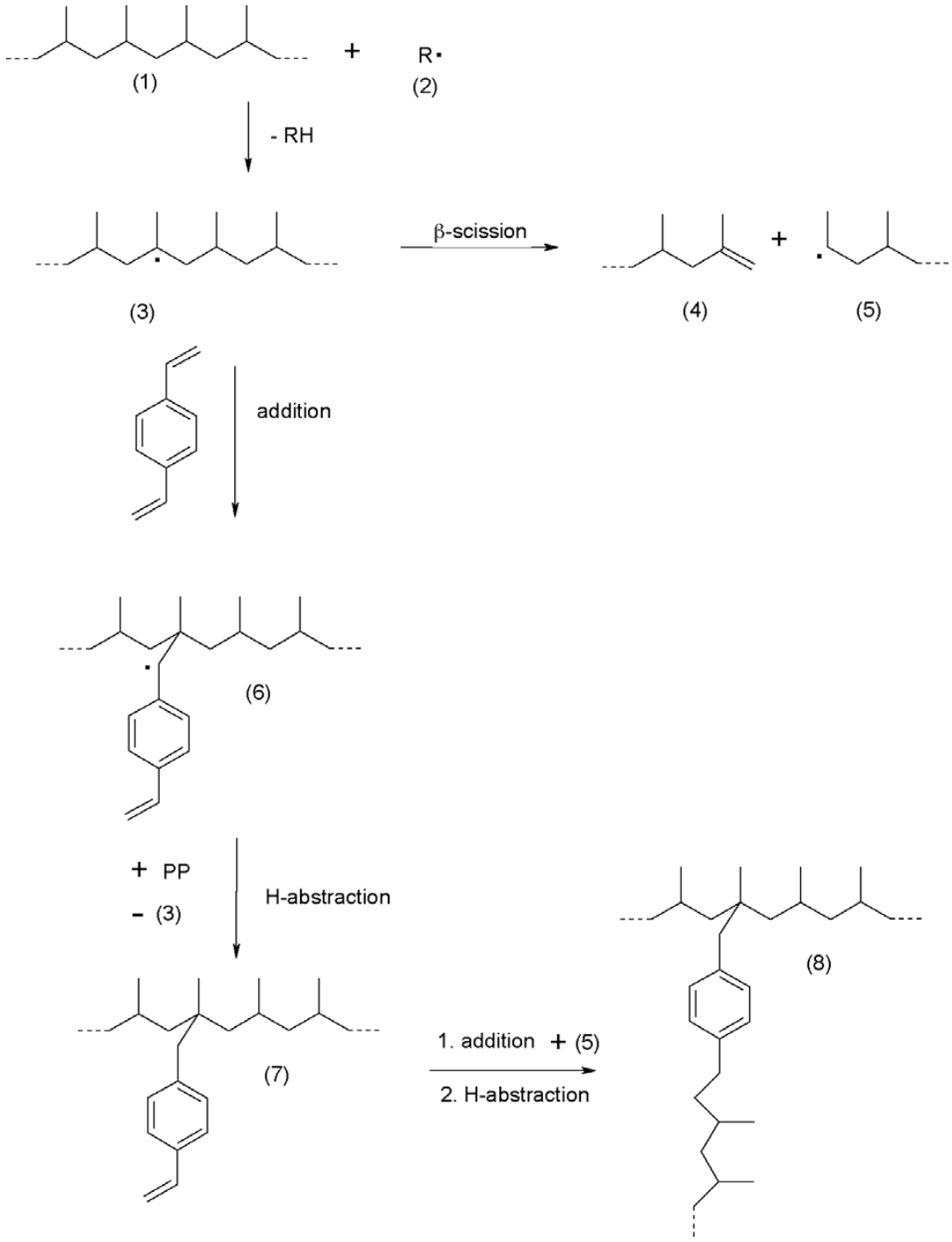

Fig. 1: Schematic presentation of the reaction mechanism involving DVB [11]

The schematic presentation of the reaction mechanism involving DVB is shown in *Fig. 1*. Primary radicals formed by the decomposition of the peroxide (2) react with iPP (1) to yield macro-radicals (3). Radicals of different reactivity (primary, secondary and tertiary) are generated, but for the sake of simplicity only tertiary ones are depicted in *Fig. 1*. These macro-radicals can, in principle, undergo β-scission of the chain end (4) and

a secondary radical (5). At the same time, the macro radicals (3) can react by addition with the unsaturated monomer (DVB) to yield the corresponding adduct (6), which can further react with the secondary macro-radical in its vicinity to form the desired LCB PP. Another route is that the adduct (6) forms the corresponding grafted product (7), i.e., PP-g-DVB, after abstraction of a hydrogen from a neighboring iPP chain. The remaining double bond on the DVB moiety of the latter can further take part in a similar formation of LCB PP [11].

1.1.2 Radical reactions

Long chain branches can be introduced by electron beam irradiation (physical method) into linear polypropylene without using polymerization facilities and special techniques or catalysts. The irradiation causes scission of linear chains followed by recombination to branched molecular structure [12]. The main oxidative reactions occurring during irradiation of a polymer resin are shown in *Fig. 2*.

$$R{-}R \rightarrow R^{\cdot} + R^{\cdot} \quad (1)$$

$$R^{\cdot} + O_2 \rightarrow RO_2^{\cdot} \quad (2)$$

$$RO_2^{\cdot} + RH \rightarrow ROOH + R^{\cdot} \quad (3)$$

$$RO_2^{\cdot} + R^{\cdot} \rightarrow ROOR \quad (4)$$

$$RO_2^{\cdot} + RO_2^{\cdot} \rightarrow ROOR + O_2 \quad (5)$$

$$ROOH \rightarrow RO^{\cdot} + {}^{\cdot}OH \quad (6)$$

$$RO^{\cdot} \rightarrow R'{=}O + R''^{\cdot} \quad (7)$$

Fig. 2: Main oxidative reactions occurring during irradiation of polymer [13]

In the processes involving polymer ionization, oxygen plays a dominant role in degradation reactions. This comes from both the oxidative chain reaction and the formation of molecular products such as hydroperoxide groups as described by reactions (2) and (3) in *Fig. 2*. These groups decompose slowly even at room temperature to re-initiate oxidation chain processes as described by reactions (6) and (7). Polymer backbone scission reaction results both from the decomposition of hydroperoxide species in alkoxyl radicals as described by reactions (6) followed by the β-scission of these radicals as described the reaction (7) and from peroxyl radicals described by reactions (2).

The chemical method contains for example the reactive extrusion of iPP with peroxydicarbonates (PODIC) or modification of iPP with peroxides in combination with multifunctional monomers. Mechanism of radical reaction is shown in *Fig. 3* [13, 14].

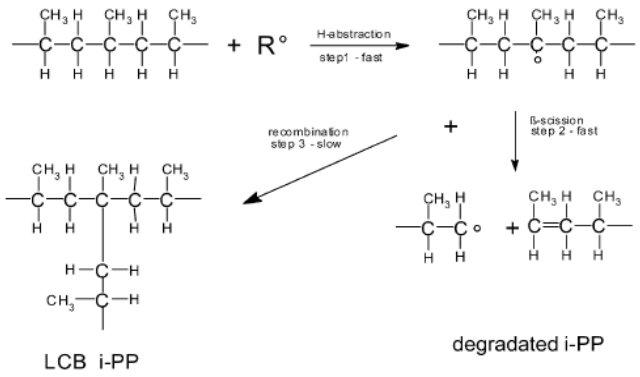

Fig. 3: LCB PP by radical reaction on iPP below 80 °C in inert atmosphere [14]

1.1.3 Heterogeneous catalysts

The one-pot process is advantaged with a simple one-step polymerization reaction, almost the same as that of regular iPP preparation. In a regular metallocene-mediated propylene polymerization, using commercial rac-$SiMe_2$[2-Me-4-(1-NaPh)Ind]$_2ZrCl_2$/ MAO catalyst, was introduced a branching agent, p-(3-butenyl)styrene (T-reagent) that in situ forms the long chain branch structure (*Fig. 4*). The catalyst maintained high activity, and the branch point density is basically proportional to the concentration of T-reagent. On the other hand, the coupling process is advantaged with the well-defined long chain branch structure. Before forming LCB structure, both backbone and side chain PP (linear) polymers are well-characterized with known polymer molecular weight and distribution, and the branch density is basically pre-determined before mixing two. Both the required chemistries to prepare maleic anhydride modified PP backbone and amino group terminated PP side chains were developed in our group [15].

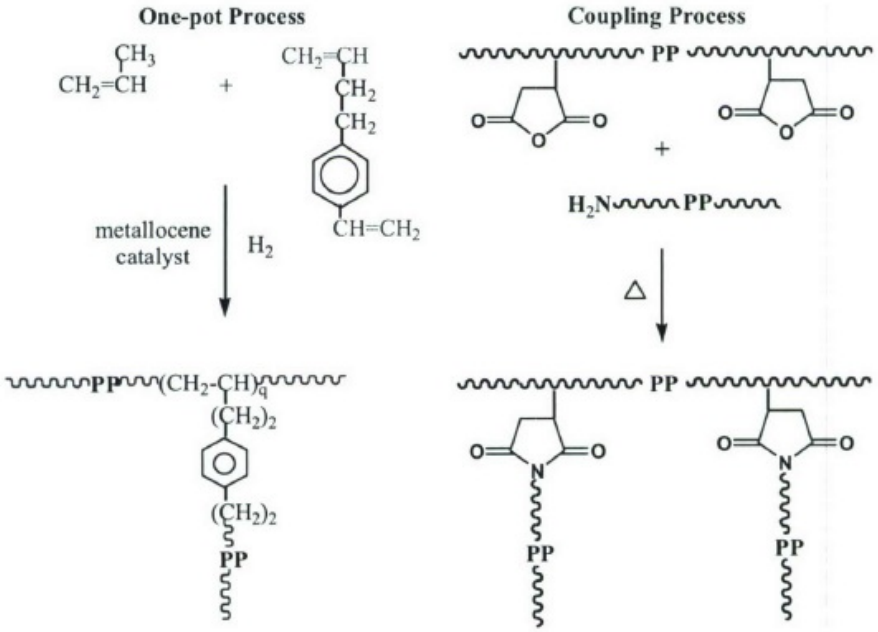

Fig. 4: Reaction mechanisms of heterogeneous catalysts [15]

1.1.4 Polymerization using peroxides

Long chain branched polypropylene can be produced by reactive extrusion with peroxydicarbonate (PODIC). All PODIC-modified samples show enhanced strain hardening, and PODIC with non-linear or large linear alkyl groups resulted in the modified PP with the highest degree of branching and the fastest strain hardening [14].

Amount of LCB can be controlled by the type and the amount of PODIC used for the modification. The peroxide structure had a direct influence on the branching level of modified iPPs. Polypropylene has a tendency to undergo β-scission because of the nature of its molecular structure, and this competes with grafting and cross-linking reactions during the reactive extrusion process [14].

When iPP is modified by peroxide and polyfunctional monomer, the reaction and the product components become very complex. Degradation reactions makes the molecular weight to decrease, grafting reaction introduced short chain branch (SCB) structure, branching reaction introduces LCB structure, and gel will be produced if cross linking reaction can happen. The complex reactions as well as the complex products make the investigation on LCB PP very difficult [16].

1.2 Properties and applications

In comparison with polyethylene, polypropylene has higher melting point, lower density, higher chemical resistance, better mechanical properties and lower cost which make this material versatile for industrial applications. Due to their low melt strength linear polypropylene cannot be used in processes where elongational properties and melt strength are dominant, such as film blowing, blow molding and foaming [17].

Long chain branched, moderately cross-linked or highly branched polymers has better rheological properties: lower Newtonian viscosity and strong shear thinning at same molecular weight, strong melt elasticity expressed by the first normal stress difference and storage modulus and enhanced strain hardening under elongational flow [18].

Long chain branched polypropylene has a wide application field. It can be used in:

- thermoformable, foamed films and sheets;
- lightweight packaging trays, beakers and containers;
- microwaveable food packaging;
- technical foams for automotive applications such as headliners, door liners, carpet backing and so on.

Foam extrusion has three specific steps comprise of:

- dissolving of a blowing agent gas in the polymer melt;
- cell nucleation;
- cell growth and stabilization.

In order to perform these additional steps, foaming extruders are longer than standard types, typically with an overall L/D ratio > 40, in either a single or tandem extruder configuration [19].

Foam extrusion of PP has lot of problems such as low bubble stability, non-controlled bubble growth and coalescence of bubbles. Product benefits of high-melt strength polypropylene with some degree of LCB in foam extrusion are contrary to conventional polypropylenes. These LCB PP resins offer both, high strength and high draw ability in the melt phase.

Typical applications of LCB PP foams are [16, 19]:

- thermo-formable foamed films, sheets and planks;
- lightweight packaging trays, beakers and containers for food packaging;

- microwaveable containers for heating of food stuff;
- thermo-formable technical foams for automotive applications.

2 CRYSTALLIZATION

Crystallization of polymers is a process which is responsible to the formation of a new crystalline phase. It occurs within the cooling polymer at the so-called nuclei upon lowering the polymer's temperature below its melting temperature. This process consists of several stages of nucleation and growth. There are essentially two major types of nucleation in polymers: homogeneous and heterogeneous.

The homogeneous nucleation which is characterized by a constant rate of nucleation stems from statistical fluctuations of the polymer chains in the melt. The heterogeneous nucleation, on the other hand, is characterized by a variable rate and a relatively low super-cooling temperature. This occurs in the presence of foreign bodies which are present in the polymer melt and which increase the rate of crystallization, acting as alien heterogeneous nuclei and reducing the free energy for the formation of a critical nucleus [20].

When semi-crystalline polymers crystallize from the melt (typically during the cooling phase of a process), the lamellae organize from a primary nucleus to form complex macro-structures called spherulites. It is widely known that these spherulites continue to grow until they impinge on an adjacent spherulite at which point the growth ceases. The ultimate size of these spherulitic structures dictates a number of properties of the polymer, including optical and physical characteristics. Additionally, for crystal growth to commence there is a primary process that has to occur, called nucleation; this is basically the formation of a focal center around which the lamellae can organize themselves. This process is displayed in *Fig. 5*. The secondary process of crystal growth follows nucleation and is characteristic for polyolefins [21].

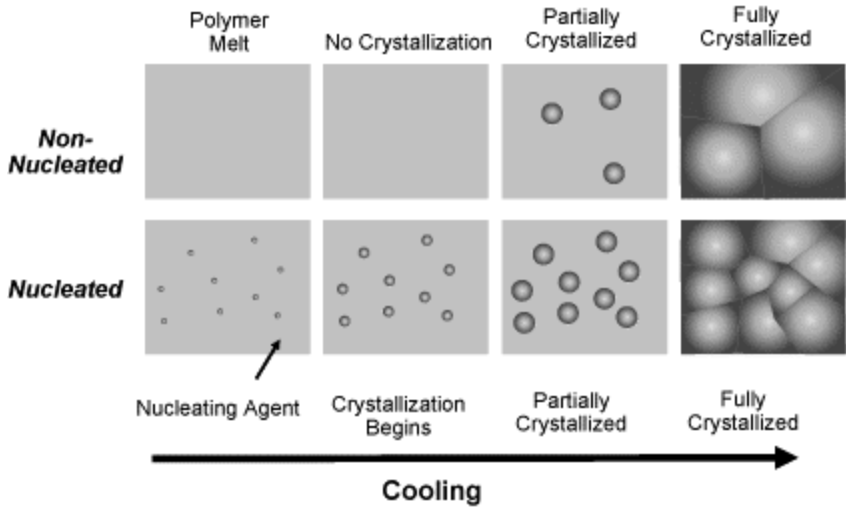

Fig. 5: Comparison of homogeneous and heterogeneous crystallization process [22]

From thermodynamic considerations alone, a crystal is in a lower free energy state than the liquid when the temperature is below the melting point for a large crystal of a very high molecular weight polymer. Crystallization adheres to Gibbs free energy [23]:

$$\Delta G=\Delta H-T\Delta S \quad (1),$$

where ΔG is change in free energy, ΔH is change in enthalpy, T is temperature and ΔS is change in entropy.

When ΔG is:

- negative → crystallization proceeds spontaneously;
- zero → system is at equilibrium;
- positive → crystallization will not proceed.

2.1 Isothermal crystallization

Quantitative characteristics of crystallization are usually determined by kinetics studies under isothermal conditions. For this purpose, changes in crystallinity with time are recorded at different crystallization temperatures. These plots are called crystallization isotherms, and they have a typical sigmoidal shape [24].

Avrami equation can specifically describe the kinetics of crystallization, can be applied generally to other change of phase in materials, like chemical reaction rates and can even be meaningful in analyses of ecological systems [25].

An equation, describing crystallization kinetics, is:

$$1-\varphi_c=\exp(-Kt^n) \quad (2),$$

where φ_c is the crystalline volume fraction developed at time t and constant temperature, and K and n are suitable parameters. K is temperature dependent. According to the original theory, n should be an integer from 1 to 4, the value of which should depend only on the type of the statistical model; however, it has become customary to regard it as an adjustable parameter that may be non-integral [26].

2.2 Polypropylene crystallization

Polypropylene can exist in different morphological forms, depending on the tacticity of the resin and the crystallization conditions, such as pressure, temperature and cooling rate. Different form can co-exist and one polymorphic form can change into another as conditions changes. There are three modifications [27]:

- *α-phase (monoclinic):* Polymer chains in the α-form of isotactic polypropylene form a helical structure in the monoclinic unit cell. Lamellae thickness is 5–20 nm. Radial growth of lamellae is dominant; however lamellae can also associate tangentially, with the tangential lamellae branching of approximately orthogonally from the plane of the radial lamellae. The α-form is the primary form of polypropylene obtained under normal processing conditions.
- *β-phase (hexagonal):* The β-form of isotactic polypropylene has a hexagonal unit cell structure (or according to Varga trigonal unit cell), with more disorder than the α-form. Polypropylene can crystallized in the β-form at specific crystallization conditions, mainly in the presence of specific nucleating agents [28–30].
- *γ-phase (orthorhombic):* The γ-form of isotactic polypropylene was initially considered to have a triclinic unit cell with dimensions similar to the α-form, but the crystal structure was recently reassigned as an orthorhombic unit cell with

nonparallel, crossed lamellae. The γ-form develops under high pressure of 200 MPa.

Each of the forms of iPP possesses different physical properties. The most thermodynamically stable α-form has the highest melting temperature and E-modulus, while β-form has significantly improved impact strength and drawability [29, 30].

2.3 Nucleating agents

Nucleating agents are chemical substances which when incorporated in plastics form nuclei for the growth of crystals in the polymer melt. In polypropylene, for example, a higher degree of crystallinity and more uniform crystalline structure is obtained by adding a nucleating agent such as adipic and benzoic acid or certain of their metal salts [31].

Generally, three classes of nucleating agents can be distinguished:

- conventional nucleating agent;
- advanced nucleating agent;
- hyper nucleating agent.

The heterogeneous nucleation is also profitably applied to improve clarity of the material. Such nucleating agents are called clarifying agents and they dramatically decrease the opacity of the polymer. For example, common clarifying agent used in polypropylene is Millad 3988, based on 1,3;2,4-bis(3,4-dimethylbenzylidene)sorbitol [22, 32, 33].

Conventional nucleating agents are the oldest nucleating agents. The most commonly used even until today are talc, sodium benzoate and aromatic carboxylic acid salts. Fillers such as talc usually induce α-form in iPP, however many organic agents also can promote the formation of α- and β-form. In some industrial application talc is preferred for its low cost. Usage of talc brings about several modifications of polypropylene properties, which increase the industrial interest for this particular composite [34].

Advanced nucleating agents are known since 1980´s and it is a newer class of nucleating agents. These have since become widely used in copolymer resins that require additional modulus enhancement and faster crystallization. Most important among these advanced nucleating agents are the phosphate ester salts [35].

Hyper nucleating agents are the most recently developed and offer processors and users the combined benefits of high crystallization rates and isotropic shrinkage control

which lead to improved production and part quality performance, in addition to the traditional mechanical property-related enhancements. Hyper nucleation technologies can also be combined to find the appropriate balance of dimensions and properties. Thus, this newest class of hyper nucleation technologies combines the main benefits of traditional nucleators whilst further optimizing performance and thus broadening the use window of polypropylene and polyethylene [36].

2.3.1 Nucleating agents for polypropylene

Application of nucleating agent in polypropylene is, together with shortening of processing time, traditionally used to improve physical properties and, in the case of some α-nucleating agents called clarifying agents, dramatically improve aesthetics of PP. Nucleating agents for polypropylene are generally divided into two groups: α-nucleating agent causing the crystallization into α-phase and β-nucleating agent for inducing formation of trigonal β-phase. The typical α-nucleating agents consist of sodium benzoate, kaolin or talc. The β-nucleating agent, are for example triphenodithiazine, pimelic acid with calcium stearate and so on [27].

The most common α-nucleating agents are sorbitol based derivates. Sorbitol based nucleators provide significant improvement over conventional nucleating agents both in nucleating efficiency and clarity. Unlike the dispersion type nucleators, they dissolve in the molten iPP and disperse uniformly in the matrix. When the iPP cools, the nucleator first crystallizes in the form of a three-dimensional fibrillar network of nanometric dimensions. The fibrils serve as nucleating sites for iPP, probably due to epitaxial growth. The most common examples of this type of nucleators are:

- 1,2,3,4-bis-dibenzylidene sorbitol (DBS);
- 1,2,3,4-bis-(p-methoxybenzylidene sorbitol) (DOS);
- 1,2,3,4-bis-(p-methylbenzylidene sorbitol) (MBDS);
- 1,3;2,4-di-(3,4-dimethylbenzylidene sorbitol) (DMDBS).

The major drawback of DBS is its fast evaporation rate during processing. Modified structures of DBS such MBDS and DMDBS have been developed to solve this problem and improve the nucleating efficiency [20].

DMDBS (trade name Millad 3988) is the most successful clarifying agent (see *Fig. 6*). When the iPP cools, the nucleator first crystallizes in the form of a three-dimensional

fibrillar network of nanometric dimensions. The nanoscale fibril network serves as nucleating sites for polypropylene, due to its large surface area, leading to enhanced nucleation of small polymer crystal [37].

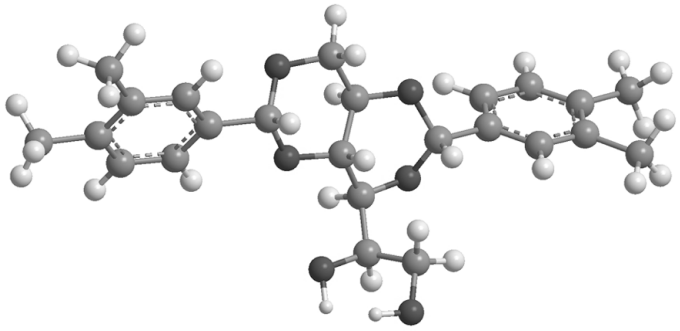

Fig. 6: Molecular structure of α-nucleating agent Millad 3988 [37]

Nucleators like DMDBS can reduce haze from 90 to 28 % in contrast to sodium benzoate, which didn´t improve optical properties. Physical and chemical properties of Millad 3988 are show in *Table 1*.

Table 1: Properties of Millad 3988 [38]

Appearance at 20 °C and 101.3 kPa	White powder
Melting point (range)	261–265 °C
Density (at 22 °C)	725 kg/m^3
Water solubility (at 22 °C)	4.76x10^{-5} g/l
Fat solubility (at 37 °C)	4.49x10^{-3} g/100g fat
Autoignition temperature	>420 °C
Particle size distribution	100 %>38 μm 67 %>300 μm

In melt-crystallized material the predominant polymorph is α-form (monoclinic). The β-form (trigonal) generally occurs at levels of only a few percent, unless certain heterogeneous nuclei are present or the crystallization has occurred in a temperature gradient or in the presence of shearing forces. β-crystals have a melting point that is generally 10–15 °C lower than that of α-crystals.

Differences between α- and β-forms of polypropylene are show in *Table 2*:

Table 2: Alpha and beta phase differences [39]

α-form	**β-form**
Melts at ~ 150 °C	Melts at ~ 150 °C
Most common phase	More ductile phase – lower forces needed for stretching
Many nucleants known	Transforms to α-form on stretching
	Undergoes more uniform drawing than α-form, and exhibits microvoiding

There are several substances that can act as β-nucleating agents: quinacridone pigments, salts of dibasic organic acids. The first effective beta nucleating agent was the γ-modification of linear trans quinacridone (LTQ). On the other hand there are many β-nucleating agents which are commercially available such as NJ Star NU-100, see *Fig. 7* [37, 40].

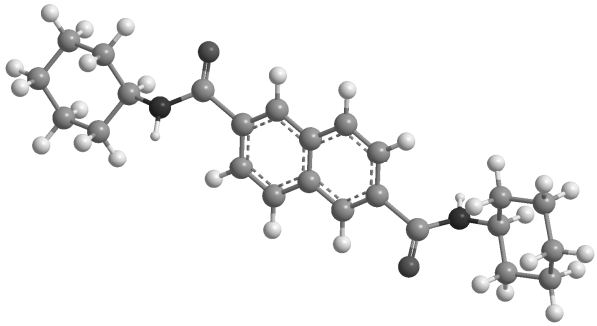

Fig. 7: Molecular structure of β-nucleating agent NJ Star NU 100; N,N'-dicyclohexylnaphthalene-2,6-dicarboxamide [37]

2.3.2 Nucleation of LCB PP

While the nucleation of isotactic polypropylene by α-nucleating/clarifying agent is well documented and widely studied [see e.g. 6-8], mainly iPP with commercial clarifying agent Millad 3988, the crystallization and properties of LCB PP modified by nucleating agents has not been overall investigated yet. Thus, this Master thesis is focused on the possible heterogeneous nucleation of LCB PP, the crystallization kinetics, morphology development and optical properties are studied.

II. EXPERIMENTAL

3 MATERIALS

3.1 Polypropylene

In this study two types of polypropylene were examined. The first one was long chain branched polypropylene Daploy WB130HMS supplied by Borealis Company. This material was produced by monomer grafting during the radical-driven reactions of iPP with peroxides to create long chain branches [42]. The next material which served as reference was linear homopolymer HC600TF supplied by Borealis Company as well. Physical properties of these two materials are summarized in *Table 3*.

Table 3: Physical properties of Daploy WB130HMS and HC600TF

Property	Test method	Unit	LCB PP	PP
Melt flow rate (230 °C; 2.16 kg)	ISO 1133	g/10min	2.0	2.8
Flexural modulus	ISO 178	MPa	1 900	1 500
Tensile strength at yield	ISO 527-2	MPa	40.0	35.0
Heat deflection temperature A	ISO 75-2	°C	60.0	85.0
Charpy impact strength (23 °C)	ISO 179/1eA	kJ/m^2	3.0	4.0

3.2 Nucleating agent

In the work α-nucleating/clarifying agent Millad 3988 based on 1,3:2,4-bis-(dimethylbenzylidene)sorbitol was applied. It is white powder with melting point 261–265 °C and its density is 725 kg/m^3 at 22 °C. The producer of the nucleating agent is Milliken Company, Belgium. The structure of Millad 3988 is shown in *Fig. 6*.

3.3 Compounding

The blend of LCB PP Daploy WB130HMS and 0.2 wt. % of clarifying agent Millad 3988 were prepared in two steps. First the nucleating agent was manually immixed into polypropylene pellets and subsequently, the blend was processed using a Brabender twin screw extruder. Before adding of nucleating agent into pellets 0.3 wt. % of paraffin oil was immixed for 10 minutes for better dispergation of the Millad 3988. After, the nucleating agent was also immixed into pellets for 10 minutes and subsequently the

mixture was compounded in twin screw extruder. Finally, the extruded rod was pelletized. The final blend composition is listed in *Table 4* and compounding conditions are summarized in *Table 5*.

Table 4: Composition of the blend

Nucleator		**Polypropylene**		**Parafin oil**			**Suma**
wt. %	**[g]**	**wt. %**	**[g]**	**wt. %**	**[g]**	**[ml]**	**[g]**
0.20	4.50	99.50	2 238.75	0.30	6.75	7.76	2 250.00

Table 5: Compounding conditions

Input sector (°C)	**Compression sector (°C)**	**Output sector (°C)**	**Frequency (min^{-1})**
180	200	210	50

4 SAMPLE PREPARATION

Plates with dimensions of 125.0x60.0x0.5 mm were compression-moulded from both virgin materials and also from prepared blend of LCB PP with nucleating agent. The material was put into preheated mould and after 5 min pressing at 210 °C the plates were cooled at 50 °C for 6 min.

4.1 Differential scanning calorimetry

For differential scanning calorimetry (DSC) cylindrical discs with diameter 5 mm were cut from the prepared plates using a hole-puncher. They were weighed, put into the aluminum pan and covered with an aluminum cover. The pan and the cover were crimped with a special toll supplied by Perking-Elmer.

4.2 Wide-angle X-ray scattering

After DSC analysis, the aluminum pans were opened and the samples were used for wide-angle X-ray scattering (WAXS).

4.3 Polarized light microscopy

Samples for polarized light microscopy (PLM) were cut using a Leica RM2255 rotary Microtome form the disc which were used for DSC and WAXS analysis. The cutting thickness was 40 μm. Samples were situated on object plate with drop of paraffin oil and were covered with micro-cover slip. They were examined at two magnitudes.

4.4 Optical properties

Samples for optical properties analysis were cut directly from compression-moulded plaques using scissors. The dimensions were 50x50 mm.

5 METHODS OF ANALYSIS

The crystallization of prepared samples was studied using differential scanning calorimetry. The morphology was observed via optical microscopy and crystallinity was calculated from wide-angle X-ray scattering patterns. Optical properties were analyzed as well.

5.1 Differential scanning calorimetry

Crystallization and melting measurements were carried out using a Perkin-Elmer Pyris 1 power-compensated differential scanning calorimeter with a nitrogen purge (20 ml/s). The temperature calibration was performed using indium. As for isothermal measurements, samples were heated from 50 do 220 °C at a heating rate of 10 °C/min, then melted at 220 °C for 5 min to erase thermal history, and subsequently cooled at 200 °C/min to the given crystallization temperature (T_c=130, 135, 140, 145 and 150 °C). The samples were annealed at crystallization temperature until the crystallization was completed. After, the samples were subjected to X-ray analysis and optical testing. Subsequently they were heated again using heating rate of 10 °C/min.

Regarding dynamic DSC scans, the process was similar to isothermal crystallization, except in cooling part when cooling rate of 10 °C/min was applied and the material was cooled to 50 °C.

5.2 Wide-angle X-ray scattering

Final structure of the samples crystallized under controlled condition in DSC was examined by wide-angle X-ray scattering. A X'PERT PRO MPD (Multi-Purposed Diffractometer) by PANanalytical Company was employed. The diffractometer is equipped with CuK_α in transmission mode and nickel filter of thickness 0.2 mm. Radial scans of intensity vs. diffraction angle 2Θ were recorded in the range of 7° to 30° by steps of 0.026°.

5.3 Polarized light microscopy

In order to observe morphology of the crystallized samples, a Zeiss NU microscope was used. Micrographs of the structure were taken using a SONY F-717 digital camera.

5.4 Optical properties

Haze of as-processed plaques was measured using a Haze-Gard Plus instrument (BYK-GARDNER Co.) according to ASTM D1003. Haze is defined as a percentage of transmitted light being scattered in an angle higher than 2.5 °.

III. RESULTS AND DISCUSSION

6 OPTICAL PROPERTIES

First of all, as-processed compression-moulded plaques of each material, i.e. long chain branched polypropylene (LCB PP), long chain branched polypropylene with nucleating agent Millad 3988 (LCB PP+NA) and linear polypropylene (PP), were subjected to optical properties testing. The results are summarized in *Table 6*. As can be seen, linear PP possesses the highest haze as could be expected. In such material homogeneous nucleation proceeds and thus relatively large spherulites could be formed. On the other hand, LCB PP shows the lowest haze. It can be concluded that the presence of long chain branches in polypropylene plays a role of clarifier and significantly decreases the haze. What is quite surprising is the higher value of haze in the case of LCB PP+NA as compared to LCB PP. Generally, the addition of clarifying agent into polypropylene leads to considerable decrease of haze. Evidently, this is not true in the case of LCB PP where, contrary, the presence of clarifying agent increases the haze nearly to the value of liner polypropylene.

Table 6: Haze of the materials

Material	Haze
PP	41.4
LCB PP	31.2
LCB PP+NA	39.3

7 NON-ISOTHERMALLY CRYSTALLIZED SAMPLES

Samples for non-isothermal crystallization were prepared as is described in Chapter 4.1. Then the melting, non-isothermal crystallization and re-melting were analyzed in differential scanning calorimeter. Before re-melting also morphology of the materials was examined via WAXS and polarized light microscopy.

7.1 Differential scanning calorimetry

From a thermograms obtained from DSC, values of melting temperature (T_m), melting enthalpy (ΔH_m), crystallization temperature (T_c), crystallization enthalpy (ΔH_c), re-melting temperature (Tm_2) and re-melting enthalpy (ΔHm_2) were analyzed. These results are listed in *Table 7*. The melting and crystallization temperatures represent the maximum of the peaks obtained from DSC thermograms.

Table 7: Results obtained from DSC for non-isothermal crystallization

Material	T_m [°C]	ΔH_m [J/g]	T_c [°C]	ΔH_c [J/g]	T_{m2} [°C]	ΔH_{m2} [J/g]
PP	164.9	93	112.9	101	161.9	93
LCB PP	158.6	90	128.8	91	159.9	94
LCB PP+NA	157.5	91	130.8	91	160.4	99

The highest melting temperature possesses linear PP (approx. 165 °C), other two materials, LCB PP and LCB PP+NA, show T_m lower of 6 and 7 °C, respectively. The melting temperature is connected with lamellae thickness, thus it could be expected that in linear PP the crystallites are more perfect with thicker lamellae [43]. The values of melting temperature of LCB PP and LCB PP+NA are quite similar. As for melting enthalpy, the values are nearly identical for all samples.

The individual melting thermograms of all samples are shown in *Figs. 8–10*. In these figures also the re-melting thermograms are plotted to compare both curves. In all cases, the melting endotherms of first melting scan show only one dominant peak corresponding to melting of α-phase (approx. 160 °C). However, the shoulders of the peaks at lower temperature can be observed. These shoulders could be connected with the presence of

trigonal β-phase within the crystal structure, even in linear polypropylene. This is not very probable in the case of LCB PP and LCB PP+NA where only α-phase is expected. On the other hand, these small peaks could also reflect the presence of two α-phases differing in the perfection of the structure [24]. However, the presence of β-phase in the samples should reveal the X-ray analysis, which is discussed thereinafter.

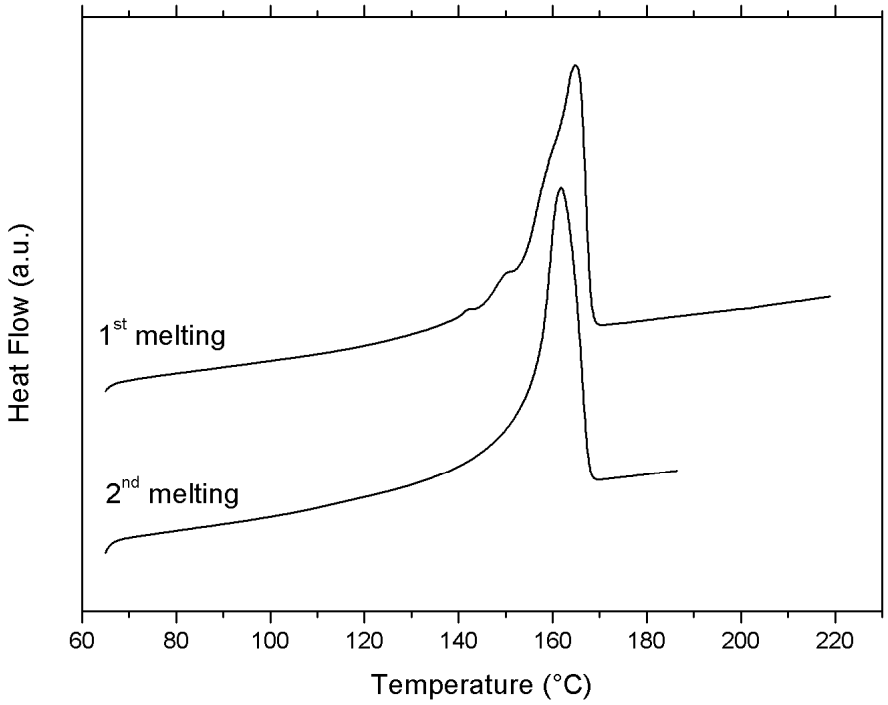

Fig. 8: Melting thermograms of PP

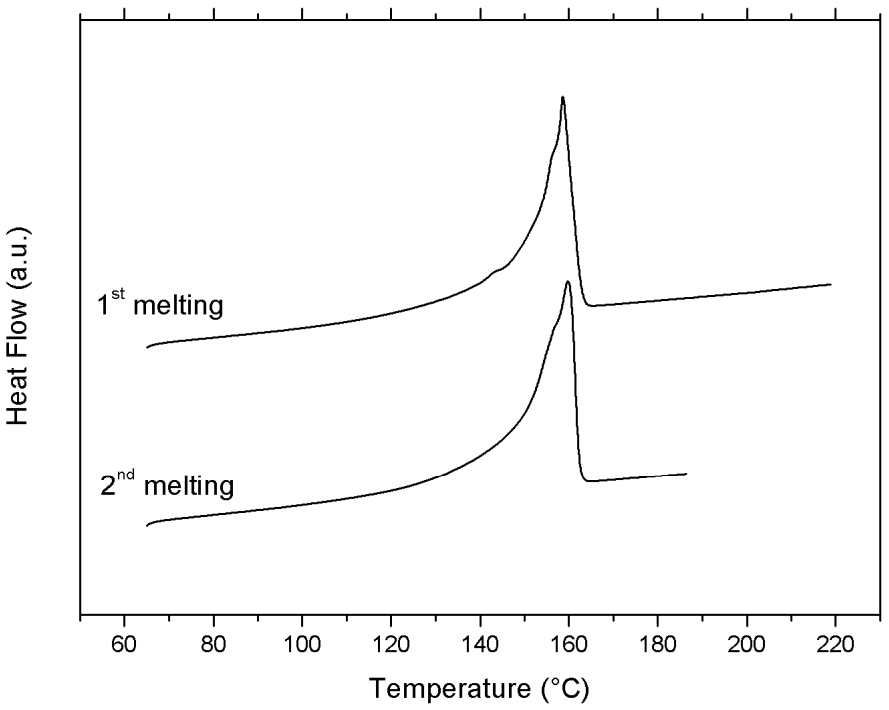

Fig. 9: Melting thermograms of LCB PP

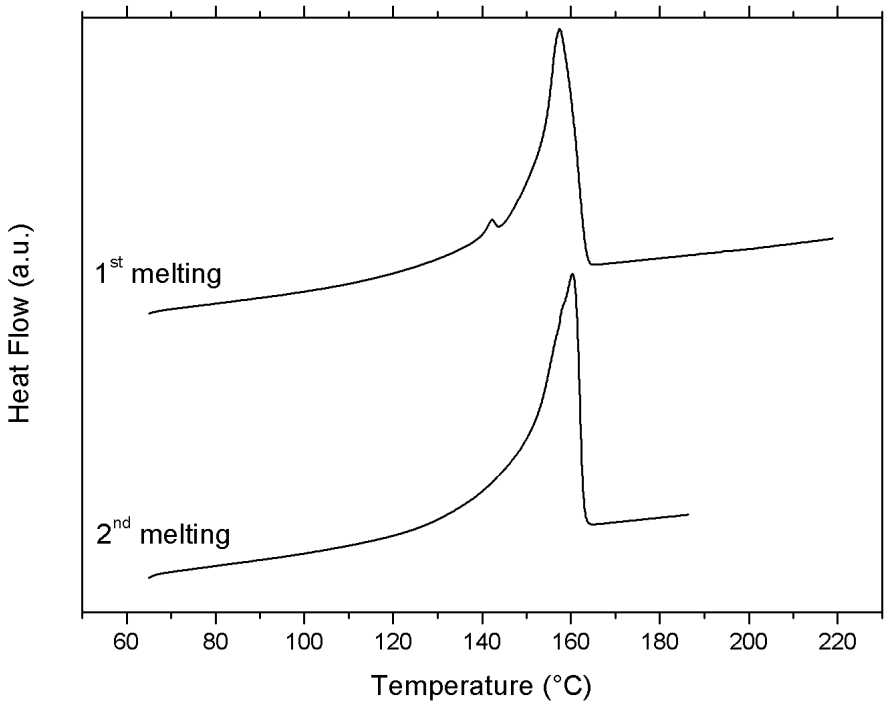

Fig. 10: Melting thermograms of LCB PP+NA

The crystallization temperature, as can be seen in *Table 7*, is the lowest in the case of linear PP (T_c=112.9 °C). The values of LCB PP and even LCB PP+NA are significantly higher, 128.8 and 130.8 °C, respectively. The difference is approx. 16 °C in LCB PP; this increase is caused by the presence of long chain branches which serves as heterogeneous nucleating agent increasing crystallization temperature, as has been already published [44]. The addition of Millad 3988 further increases the value of T_c of 2 °C, however, such increase is not that much significant. The values of crystallization enthalpy of all samples are again quite similar; the value of linear PP is somewhat higher. Nevertheless, these values correlate with the values of melting enthalpy.

The crystallization exotherms of all samples are shown in *Fig. 11*. Here, the dramatic increase of crystallization temperature in LCB PP and LCB PP+NA can be clearly observed. Moreover, the exotherms of LCB PP and LCB PP+NA are symmetrical while that one of linear PP is deformed. This points to the faster and more regular crystallization in LCB PP and LCB PP+NA.

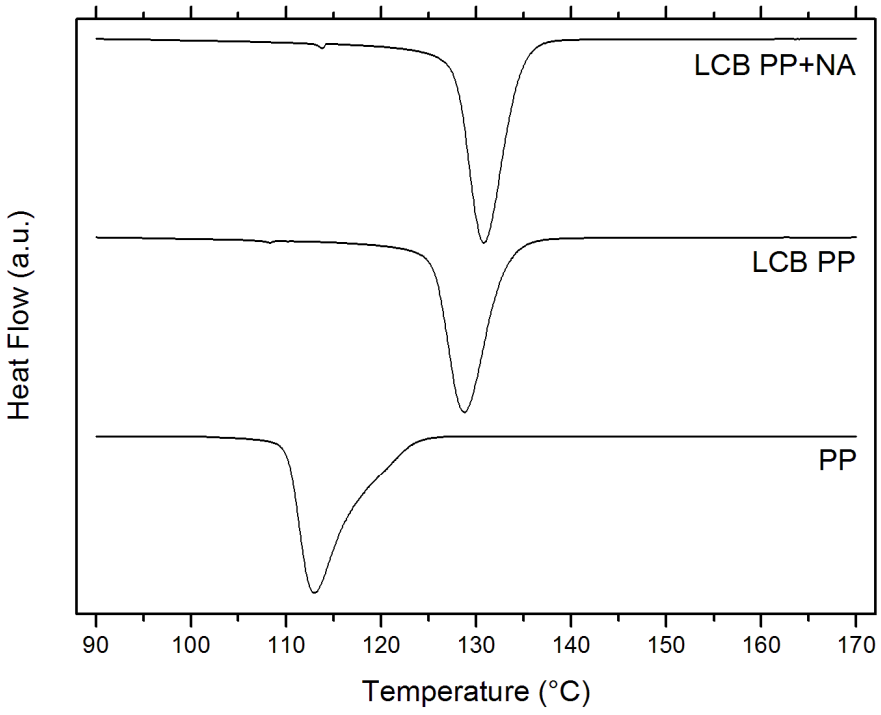

Fig. 11: Crystallization exotherms of the samples

Table 7 also shows the values of re-melting temperatures and re-melting enthalpy. These values are very similar for all samples. The re-melting endotherms are plotted in *Figs. 8–10*. As compared to first melting scans no shoulders (or neglectable) can be observed. Thus the structure formed during controlled crystallization in DSC is more uniforms as compared to the structure formed during sample preparation in manual press.

7.2 Wide-angle X-ray scattering

The crystallinity and polymorphic composition of the non-isothermally crystallized samples were analyzed using wide-angle X-ray scattering. The crystallinity was calculated from WAXS patterns as the ratio of the integral intensities diffracted by a crystalline part (I_c) and total integral intensities (I): $X=I_c/I$. The individual values are listed in *Table 8*. It can be seen that linear PP possesses the highest value of crystallinity while the lowest one shows LCB PP. The addition of Millad 3988 into the LCB PP leads to significant increase of crystallinity of 8 % more. The values of crystallinity obtained from WAXS do not fully correspond to the values of crystallization and re-melting enthalpy from DSC which can be used for crystallinity determination. Nevertheless, the data obtained from WAXS have a better relevance since they are not such dependent on human factor during evaluating and moreover on re-crystallization processes which can occur during DSC measuring.

Table 8: Crystallinity of non-isothermally crystallized samples

Material	Crystallinity (%)
PP	70
LCB PP	59
LCB PP+NA	67

Fig. 12 shows WAXS patterns obtained for all the non-isothermally crystallized samples. The typical diffraction peaks associated with α-phase can be observed at angles 2θ=14.2, 17 and 18.8 °. No β-diffraction peat (at 2θ=16.2 °) is observed. Thus, only α-phase has been formed in all the materials.

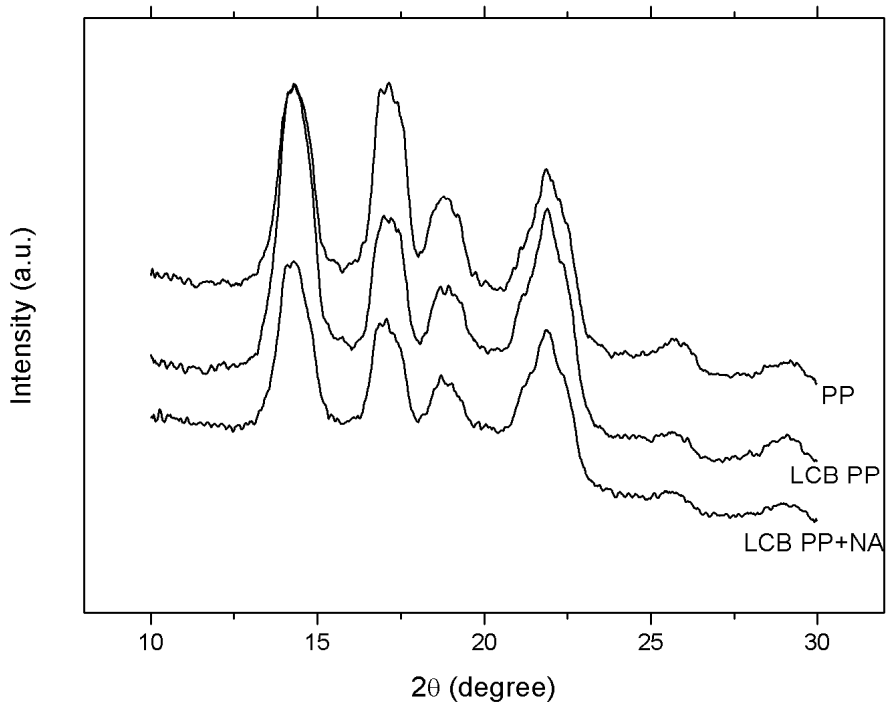

Fig. 12: WAXS patterns of all non-isothermally crystallized samples

7.3 Polarized light microscopy

Polarized light microscopy was used to directly observe structure formed during controlled non-isothermal crystallization in DSC. It can be clearly seen in *Figs. 13* and *14* that linear PP shows typical spherulitical structure: the spherulites are quite large and very well observed. On the other hand, the spherulites cannot be distinguished in other two samples. The crystalline objects in these samples are too small to be observed in polarized light microscopy. This is caused by the fact that the long chain branches serves as heterogeneous nucleating agent increasing the number of crystallites and thus significantly decreasing their size [45]. The structure of LCB PP and LCB PP+NA is very similar. For more detailed analysis of the structure another method should be used, such as scanning electron microscopy.

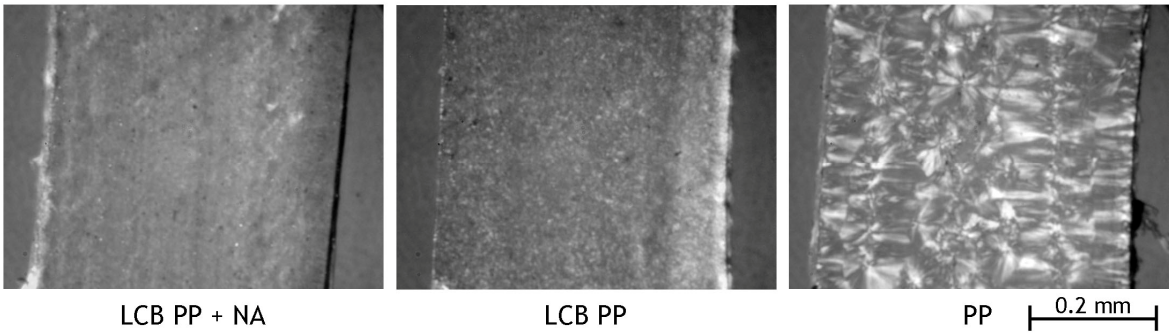

Fig. 13: Micrographs of the non-isothermally crystallized samples; low magnitude

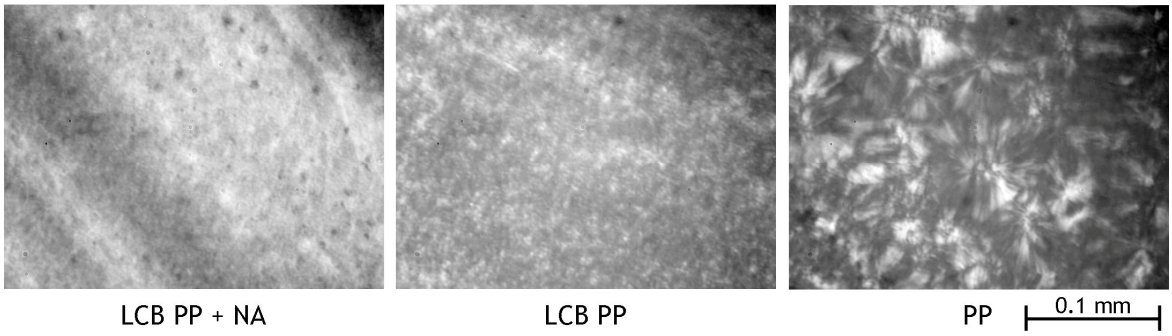

Fig. 14: Micrographs of the non-isothermally crystallized samples; high magnitude

8 ISOTHERMALLY CRYSTALLIZED SAMPLES

Samples for isothermal crystallization were prepared as is described in Chapter 4.1. Then isothermal crystallization at several temperatures ranging from 130 to 150 °C and subsequent melting were analyzed in differential scanning calorimeter. Before re-melting also morphology of the materials was examined via WAXS and polarized light microscopy. The kinetics of isothermal crystallization was evaluated according to Avrami.

8.1 Differential scanning calorimetry

The results obtained from DSC analysis are listed in *Table 9*. In this table Avrami parameters n and K, halftime of crystallization $t_{1/2}$, crystallization enthalpy ΔH_c, melting temperature T_m and melting enthalpy ΔH_m are shown.

Table 9: Result from isothermal DSC analysis: crystallization and melting characteristics

Material	T_c [°C]	n [-]	K [-]	$t_{1/2}$ [min]	ΔH_c [J/g]	T_m [°C]	ΔH_m [J/g]
PP	130	1.84	$1.51x10^{-4}$	1.8	80	163.3	108
	135	2.04	$6{,}01x10^{-6}$	5.1	106	164.7	107
	140	1.97	$5.93x10^{-7}$	20.3	110	167.4	108
	145	1.94	$1.38x10^{-7}$	48.9	111	170.8	107
	150	1.66	$1.04x10^{-7}$	55.4	118	175.1	113
LCB PP	130	-	-	-	-	159.3	98
	135	-	-	-	-	160.0	89
	140	-	-	-	-	161.5	92
	145	2.23	$1.56x10^{-5}$	2.0	75	161.0	93
	150	2.39	$3.09x10^{-7}$	7.6	83	164.4	91
LCB PP+NA	130	-	-	-	-	159.1	100
	135	-	-	-	-	160.4	95
	140	-	-	-	-	160.7	93
	145	1.88	$1.00x10^{-7}$	2.2	84	161.2	95
	150	2.87	$5.34x10^{-8}$	5.6	81	163.7	86

In the case of LCB PP and LCB PP+NA crystallized at relatively low crystallization temperatures (namely 130, 135 and 140 °C) no Avrami characteristics and crystallization enthalpy is shown. This is caused by fast crystallization which started even before achievement crystallization temperature. Thus the crystallization peaks were not complete and it was not possible to evaluate Avrami kinetics of crystallization.

To evaluate Avrami equation not all obtained data of crystallization curve (percentage of crystallized phase vs. time) were used. Only the data from 20 to 80 % crystallized phase were used since the ending data could misrepresent the results.

It can be seen in *Table 9* than Avrami exponent reaches the values approx. 2 in all cases. However, the values are fractional. In polymer crystallization from an entangled melt, non-integer values of are often obtained, indicative of an overlap of different crystal growth geometries [46]. The rate constant K from Avrami equation shows decreasing tendency with increasing crystallization temperature in all cases of material. This is well known fact well described in literature.

The crystallization halftime which is defined as a time at which the extent of crystallization is 50 % completed can be used to describe the rate of crystallization; long crystallization halftime corresponds to a slow crystallization rate. It can be seen in *Table 9* that in the case of linear PP the crystallization halftime dramatically increases with the increasing crystallization temperature while the crystallization rate decreases as could be expected. In the case of LCB PP and LCB PP+NA only two values of $t_{1/2}$ could be evaluated for T_c = 145 and 150 °C, however in both cases the $t_{1/2}$ is lower for higher T_c. The addition of Millad 3988 into LCB PP slightly speeds the crystallization rate as the values of $t_{1/2}$ of LCB PP+NA are somewhat lower.

Table 9 also summaries the values of crystallization enthalpy ΔH_c. As can be seen the values of ΔH_c increase with increasing crystallization temperature what is especially evident in the case of linear PP for which all the values could be evaluated. Only one exception is LCB PP+NA; here the value of ΔH_c is slightly higher for lower crystallization temperature. Such difference is nevertheless very small and the values are comparable. This tendency points to increasing crystallinity with increasing crystallization temperature and such prediction can be proved via WAXS experiment which is discussed thereinafter in the text.

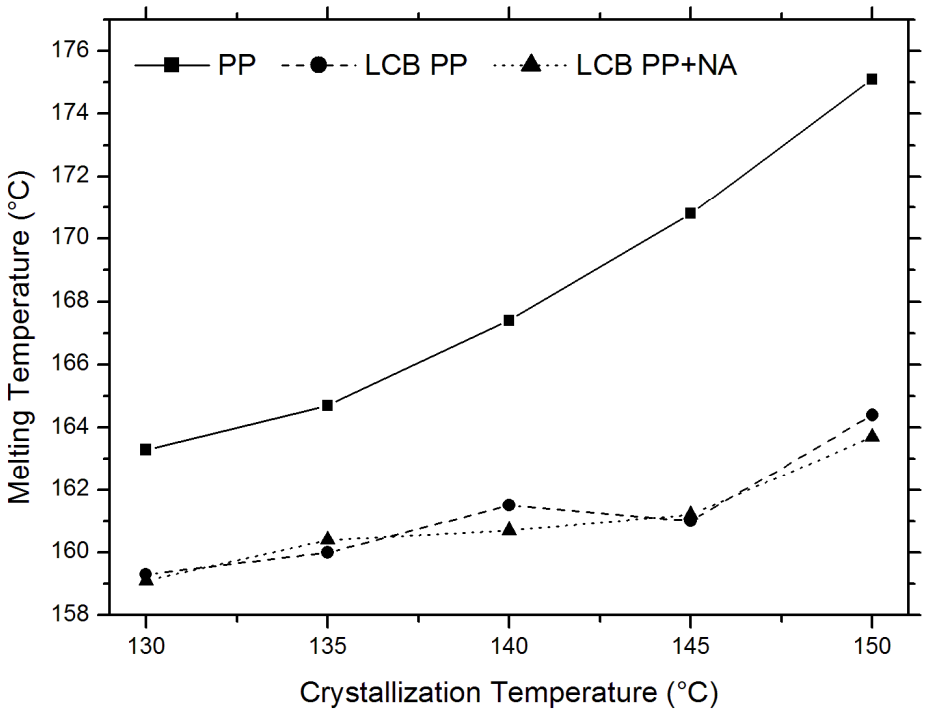

Fig. 15: The dependence of melting temperature on crystallization temperature at which the samples crystallized

The last characteristic which is listed in *Table 9* is melting temperature of isothermally crystallized materials. The dependence of melting temperature on crystallization temperature at which the samples crystallized is shown in Fig. 15. It can be observed that linear PP possesses significantly higher melting temperatures as compared to other two materials. The values of melting temperatures of LCB PP and LCB PP+NA are similar. Thus the addition of Millad 3988 does not significantly influences the structure formed during isothermal crystallization of LCB PP. What is also observed is increasing tendency of T_m with increasing crystallization temperature. This trend is observed for all the samples. This is connected of creation of more perfect structure during slow crystallization at higher T_c.

Figs. 16–20 show the crystallization exotherms formed during crystallization at different T_c. In each figure the crystallization exotherms of all three materials are compared. In all figures the significant difference in the exotherms of linear PP and LCB PP (resp. LCB PP+NA) can be observed. Linear PP shows broad peak while other

two materials show sharp peak which is finished in very short time. The peak is even sharper in the case of LCB PP+NA than LCB PP. These results correspond to the Avrami characteristics listed in *Table 9*. It can be also seen in the *Figs. 16–18* that the crystallization peaks of LCB PP and LCB PP+NA are not complete; the onset of the peak is not recorded due to very fast crystallization which proceeds even during fast cooling to crystallization temperature. Another feature which is observed is the deformation of crystallization exotherms of linear PP. Thus the crystallization does not proceed fluently and the rate of crystallization changes with time.

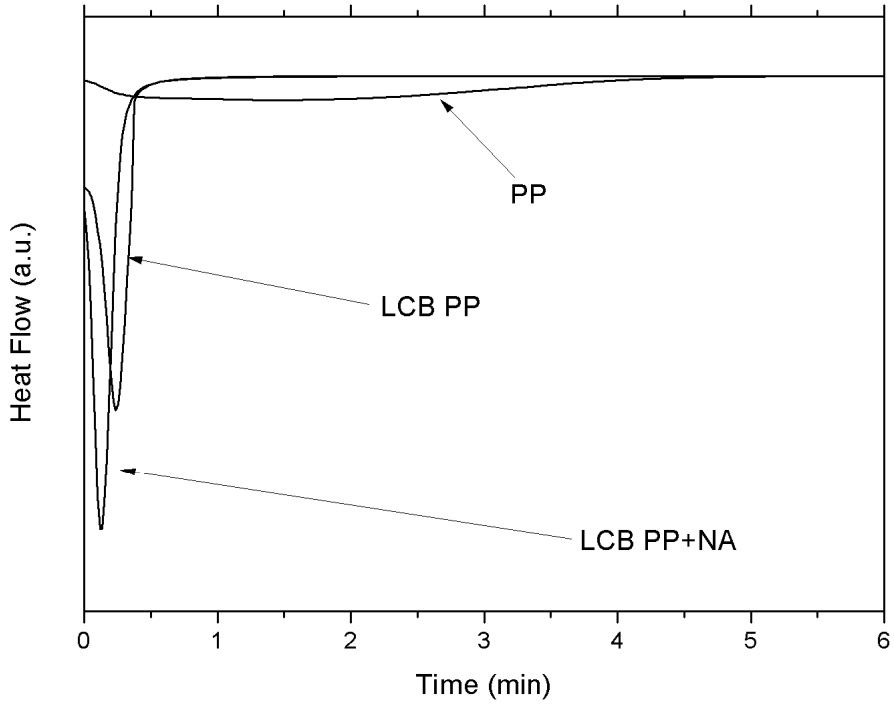

Fig. 16: Crystallization exotherms of isothermally crystallized samples at 130 °C

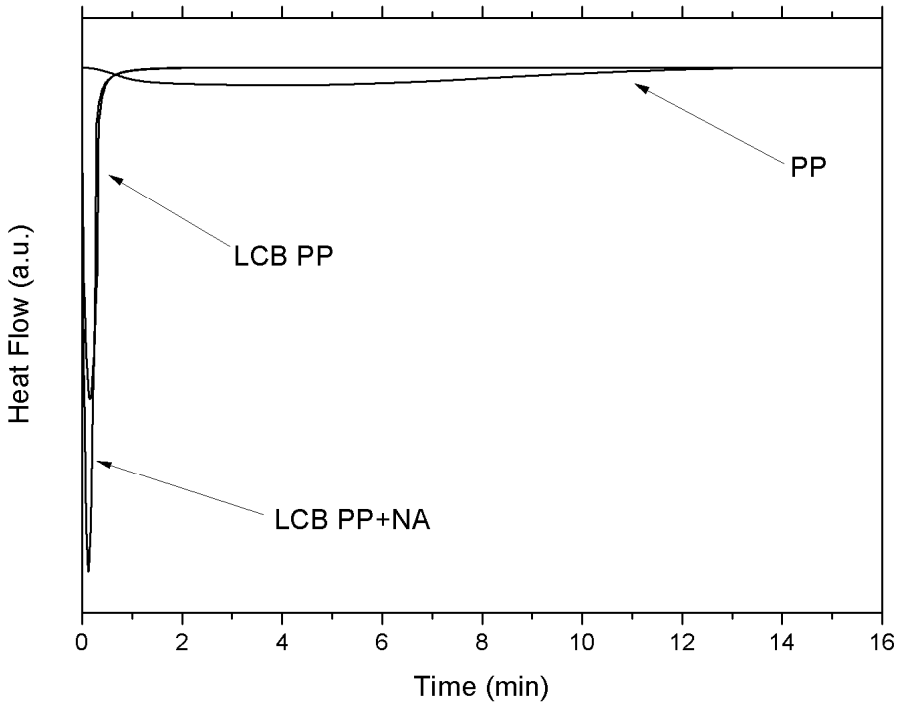

Fig. 17: Crystallization exotherms of isothermally crystallized samples at 135 °C

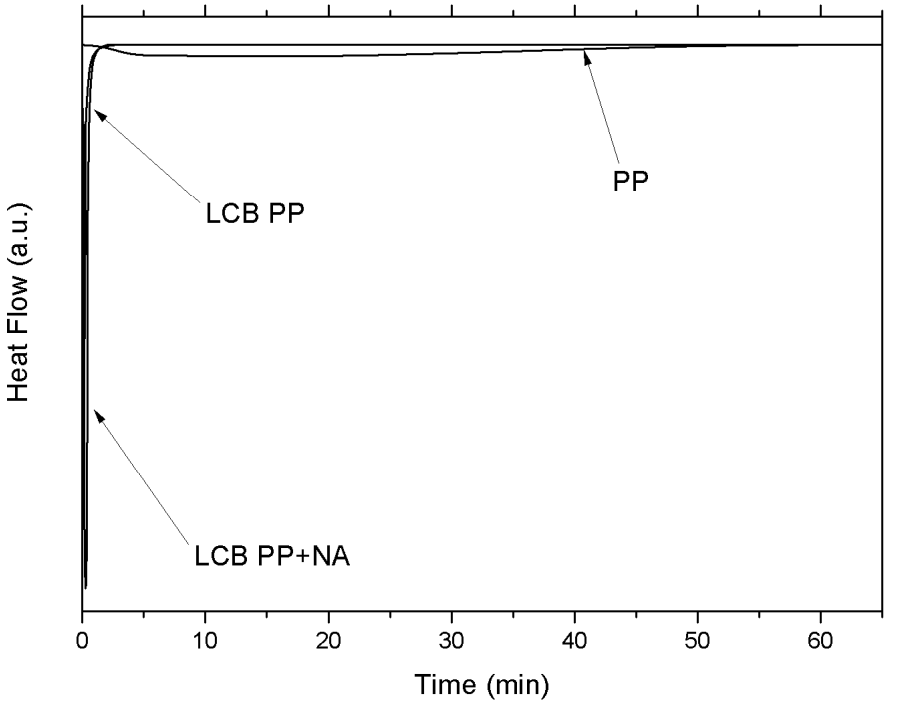

Fig. 18: Crystallization exotherms of isothermally crystallized samples at 140 °C

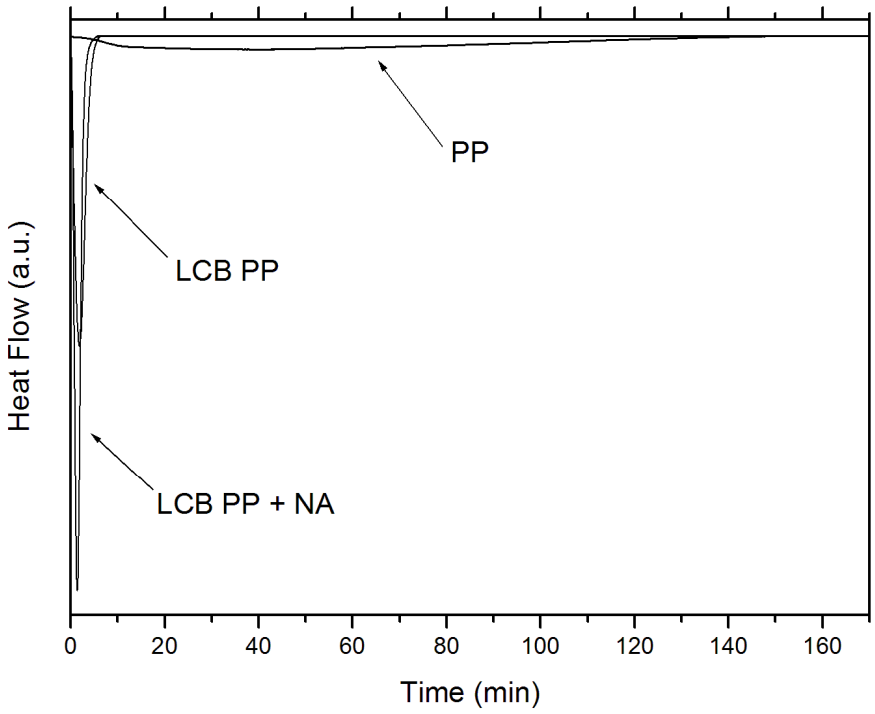

Fig. 19: Crystallization exotherms of isothermally crystallized samples at 145 °C

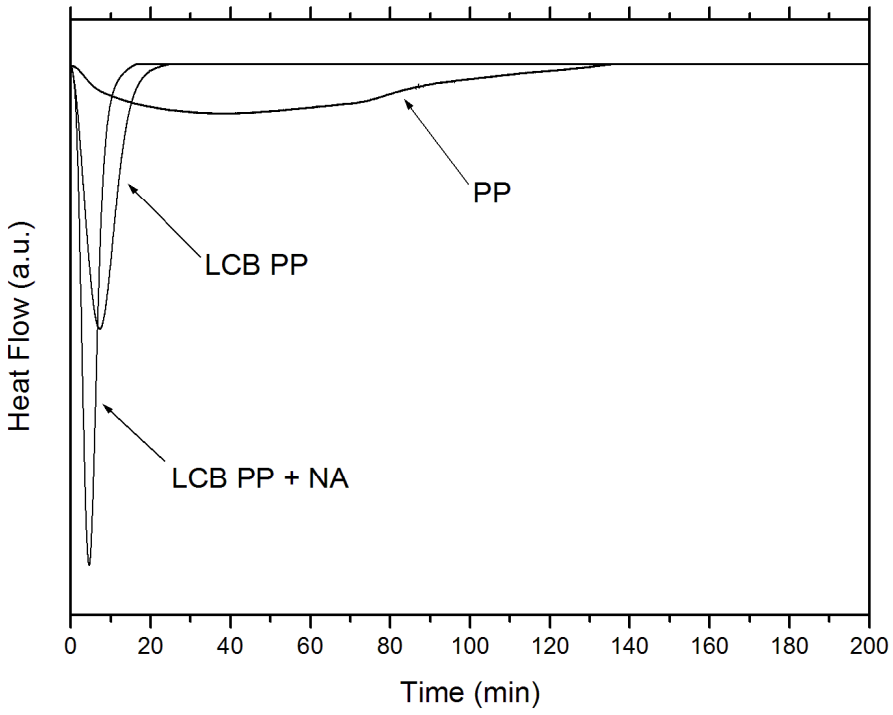

Fig. 20: Crystallization exotherms of isothermally crystallized samples at 150 °C

The crystallization exotherms of individual materials formed at different crystallization temperatures are compared in *Figs. 21–23*. In these figures the gradual prolongation of crystallization time with increasing crystallization temperature is clearly seen. The crystallization exotherm becomes broader and shallower with higher T_c in all cases. Corresponding crystallization curves (relative crystallinity vs. time) are plotted in *Figs. 24–26*. The curves were obtained via integration of exothermic peaks. In the case of LCB PP and LCB PP+NA only the curves connected to T_c 145 and 150 °C are shown since the others could not be evaluated due to non-complete crystallization exotherms what was discussed earlier in the text. It can be seen it these figures that the crystallization curves possesses typical sigmoid shape. The prolongation of $t_{1/2}$ with increasing T_c is evident.

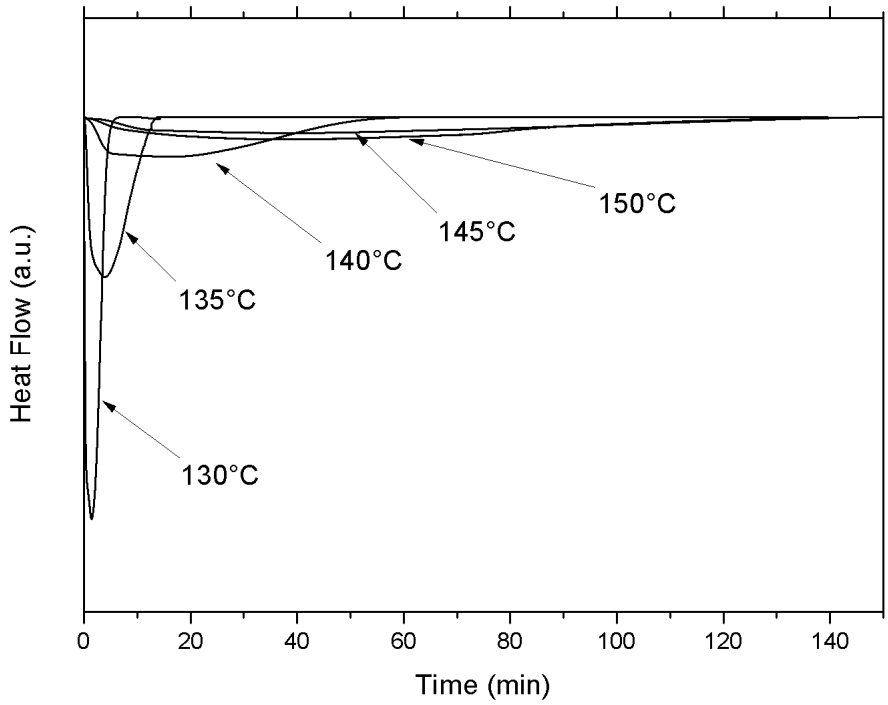

Fig. 21: Crystallization exotherms of linear PP isothermally crystallized at different temperatures

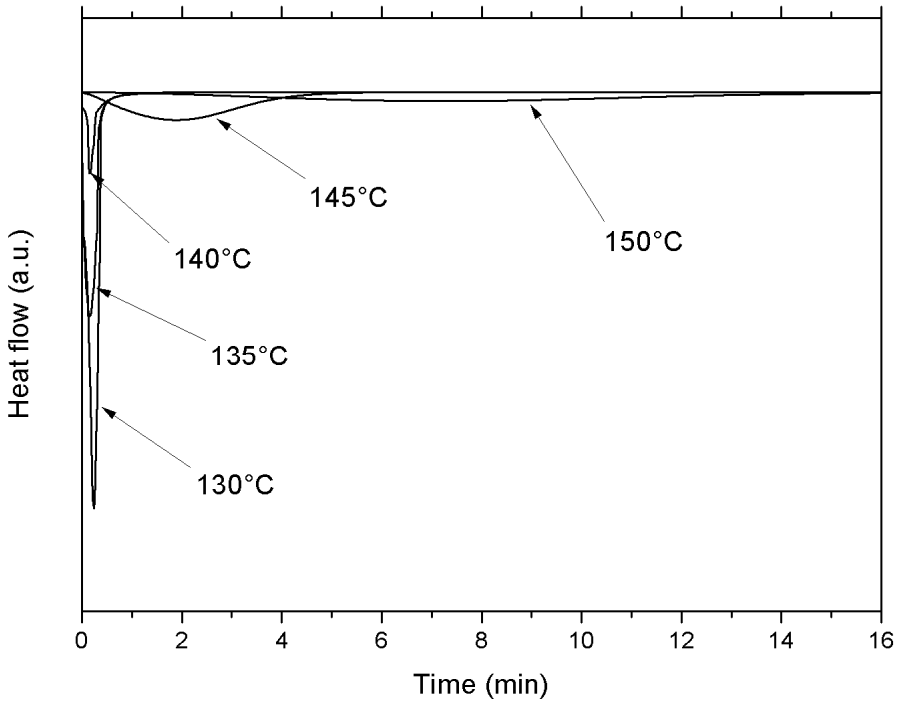

Fig. 22: Crystallization exotherms of LCB PP isothermally crystallized at different temperatures

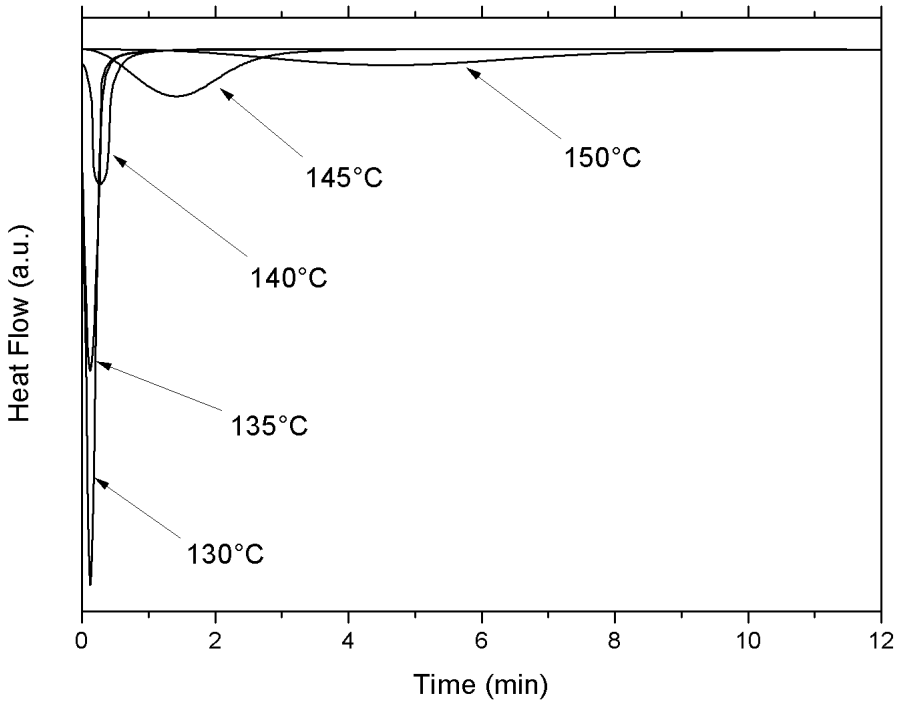

Fig. 23: Crystallization exotherms of LCB PP+NA isothermally crystallized at different temperatures

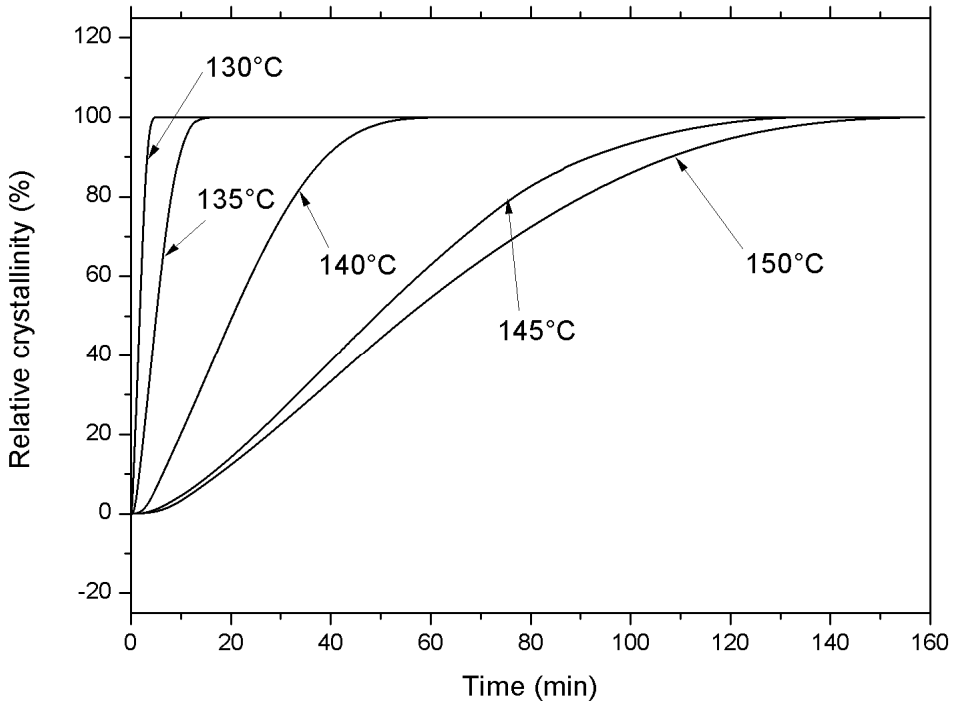

Fig. 24: Crystallization curves of linear PP isothermally crystallized at different crystallization temperatures

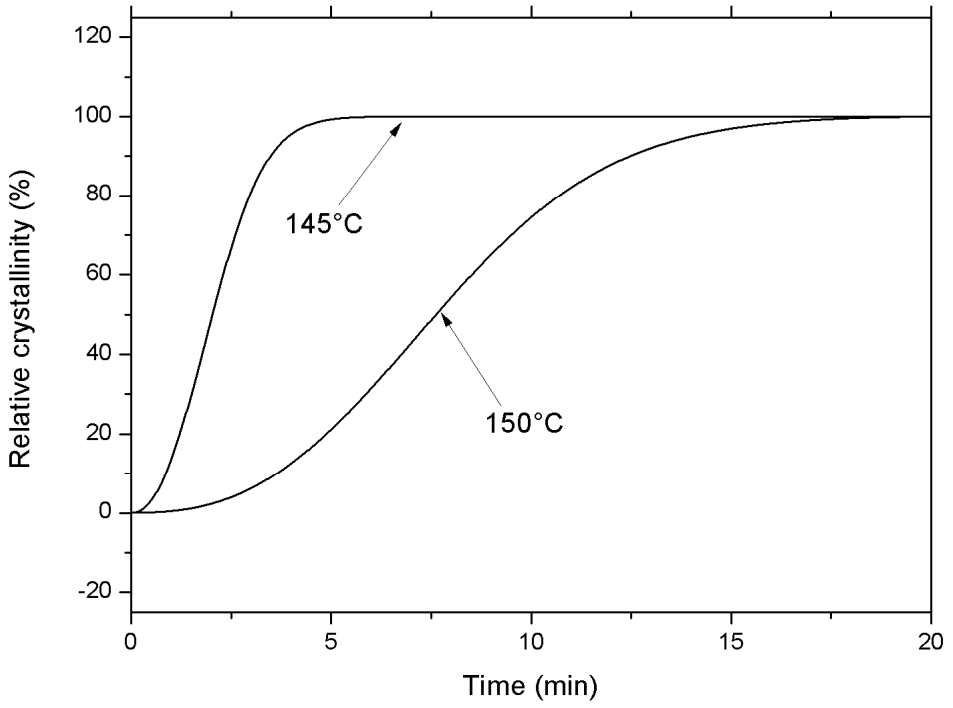

Fig. 25: Crystallization curves of LCB PP isothermally crystallized at different crystallization temperatures

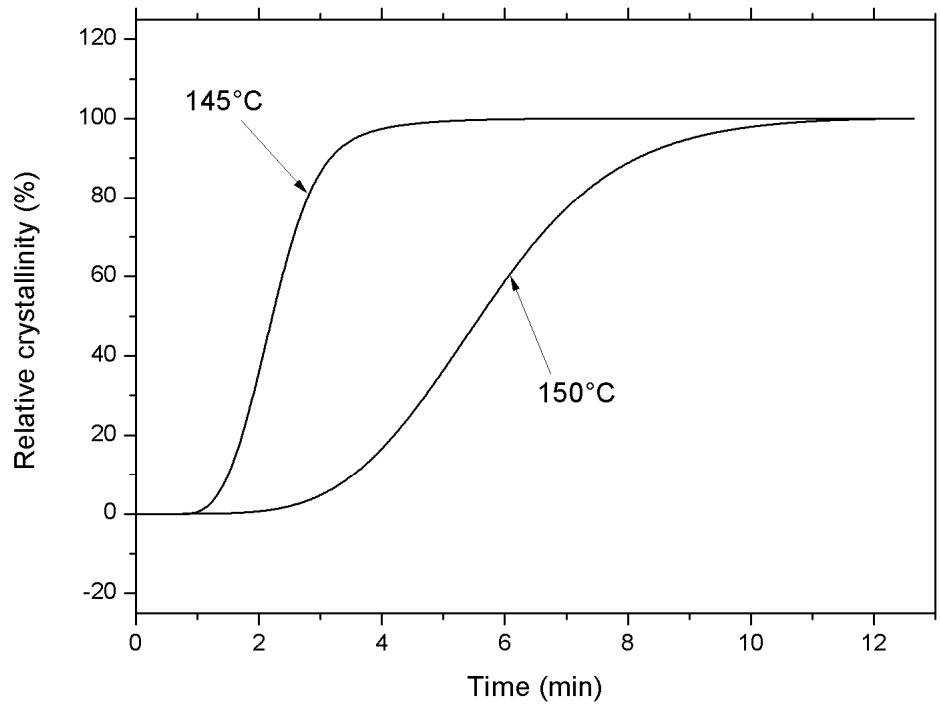

Fig. 26: Crystallization curves of LCB PP+NA isothermally crystallized at different crystallization temperatures

The melting endotherms of isothermally crystallized materials are shown in *Figs. 27–29*. It can be seen in *Fig. 27* that melting curve of linear PP crystallized at low T_c (130 and 135 °C) consists only of one melting peak corresponding to melting of α-phase. The increase of T_c then causes broadening of melting peak leading to creation of the shoulder and finally at the highest T_c second individual peak. This splitting of melting peat into two peaks might be caused by the formation of two crystalline phases during crystallization: These two phases have different thermodynamical stability. The creation of two phases is also proved by formation of deformed crystallization peak during isothermal crystallization of linear PP (see *Fig. 21*).

The formation of the shoulder of melting peak is also observed in the case of LCB PP (see *Fig. 28*). However, here the shoulder is not as significant as in previous case (linear PP). The distinct shoulder is not observed in melting thermograms of LCB PP+NA (see *Fig. 29*).

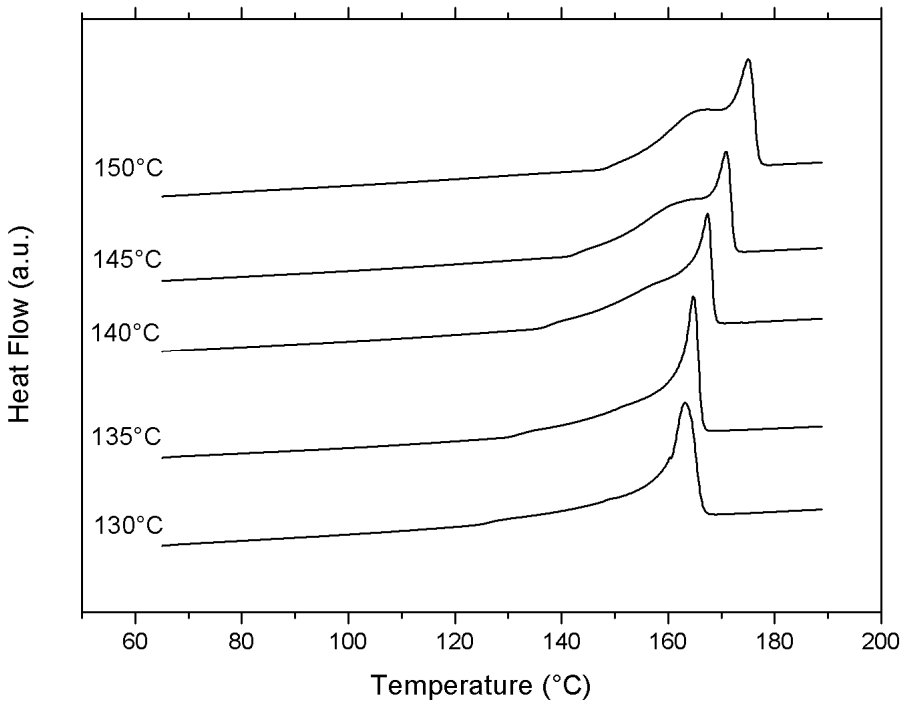

Fig. 27: Melting endotherms of linear PP isothermally crystallized at different crystallization temperatures

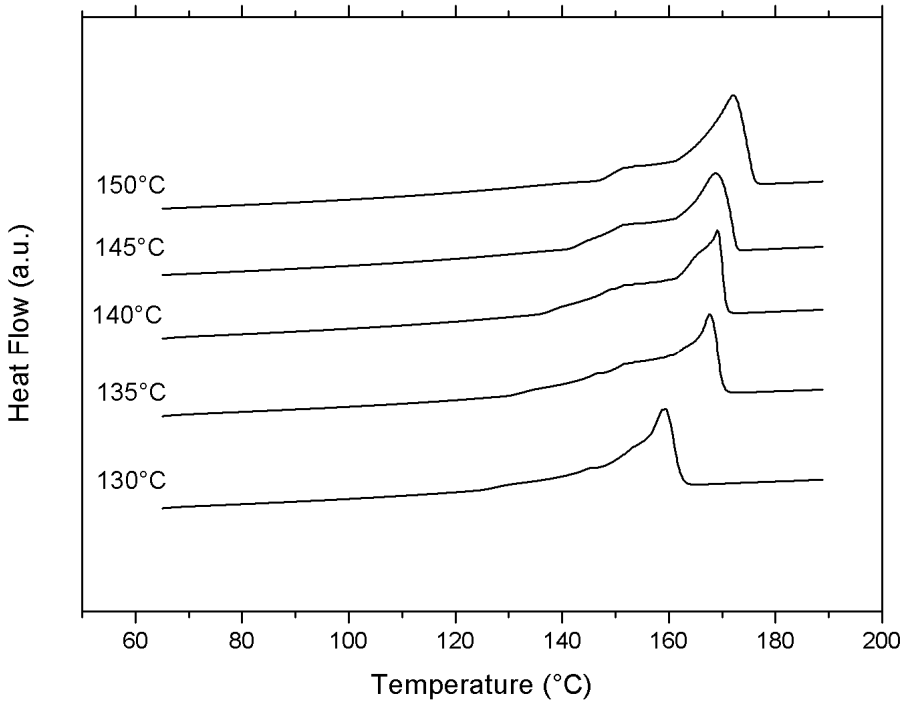

Fig. 28: Melting endotherms of LCB PP isothermally crystallized at different crystallization temperatures

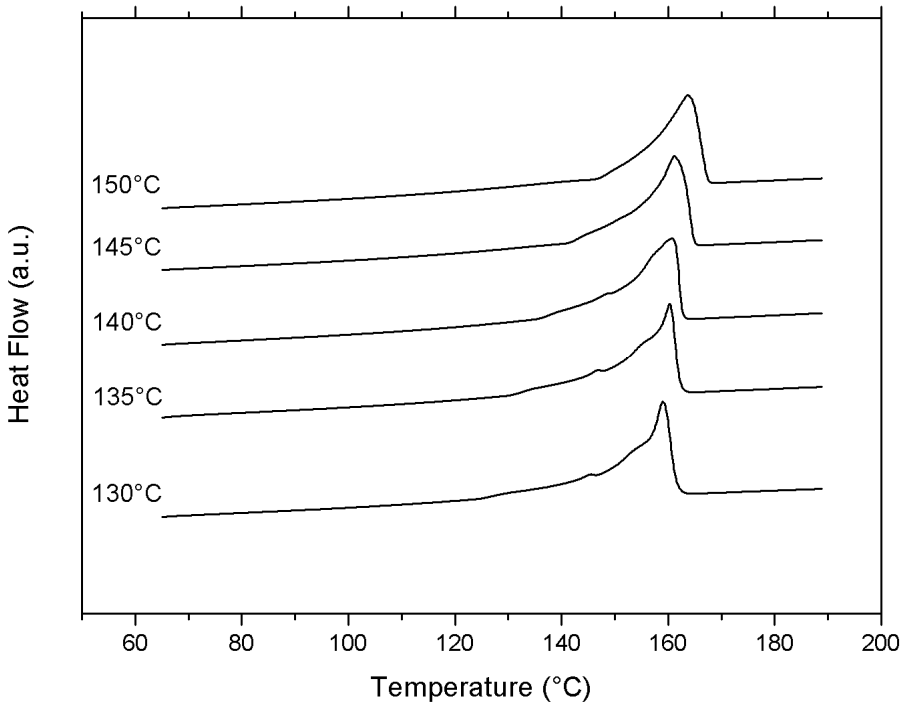

Fig. 29: Melting endotherms of LCB PP+NA isothermally crystallized at different crystallization temperatures

8.2 Wide-angle X-ray scattering

The values of crystallinity of isothermally crystallized samples were calculated from WAXS patterns as described earlier in the text (Chapter 7.2). The results are listed in *Table 10* and graphically expressed in *Fig. 30*. Individual WAXS patterns are shown in *Figs. 31–33*.

Table 10: Crystallinity values of isothermally crystallized samples

T_c [°C]	PP	LCB PP	LCB PP+NA
	[%]		
130	70	67	65
135	70	68	65
140	73	71	66
145	80	72	63
150	82	72	76

It is clear from *Fig. 30* that linear PP possesses the highest values of crystallinity among all the material. This corresponds with the crystallization enthalpy values obtained from DSC analysis (see *Table 9*). The lowest values of crystallinity show LCB PP+NA. The overall trend with increasing T_c is increasing and such result also corresponds with DSC data. Only one yawing value which can be observed is 63 % of crystallinity of LCB PP+NA crystallized at 145 °C. This could be taken as a mistake in measurement. The increasing crystallinity with increasing T_c was expected; the slower crystallization enables better crystallites organization.

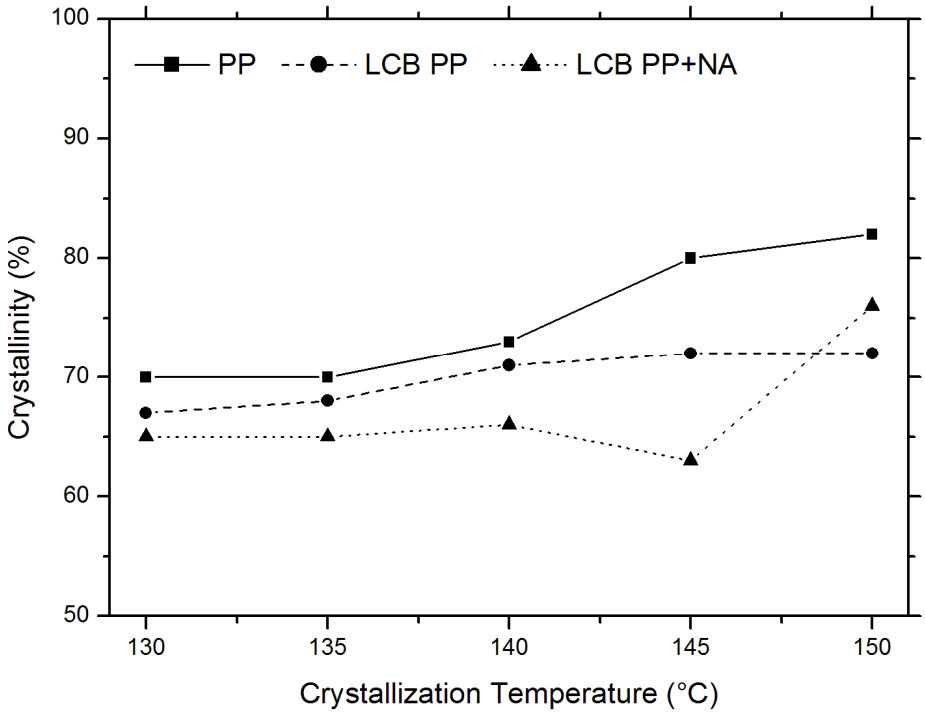

Fig. 30: The dependence of crystallinity of isothermally crystallized samples on crystallization temperature

WAXS patterns reveal that only α-phase was formed during isothermal crystallization in all samples see *Figs. 31–33*. Typical diffraction peaks for α-phase are observed while β-diffraction peak is not visible.

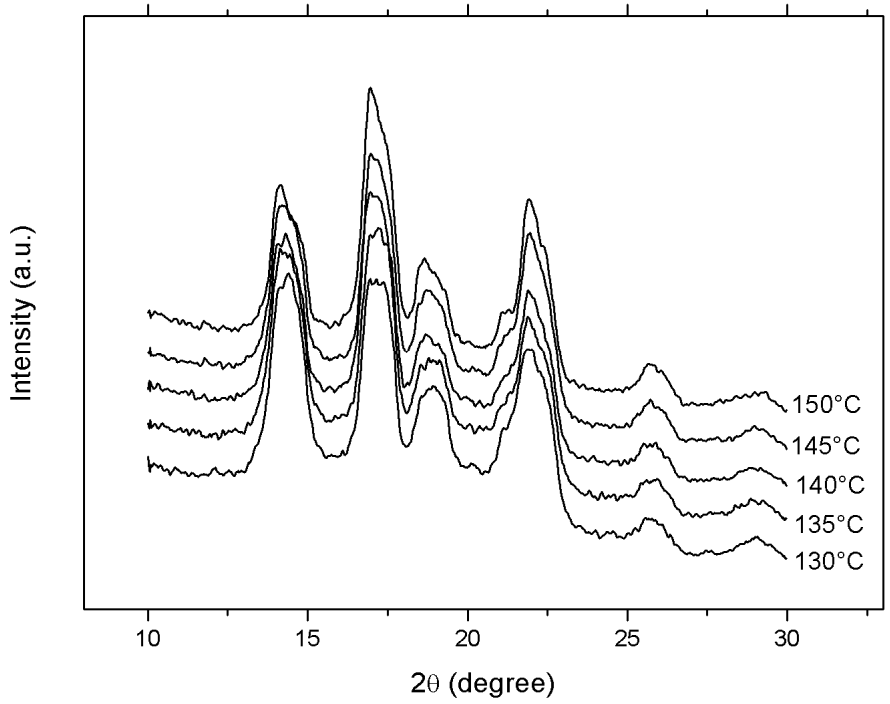

Fig. 31: WAXS patterns of linear PP isothermally crystallized at different crystallization temperatures

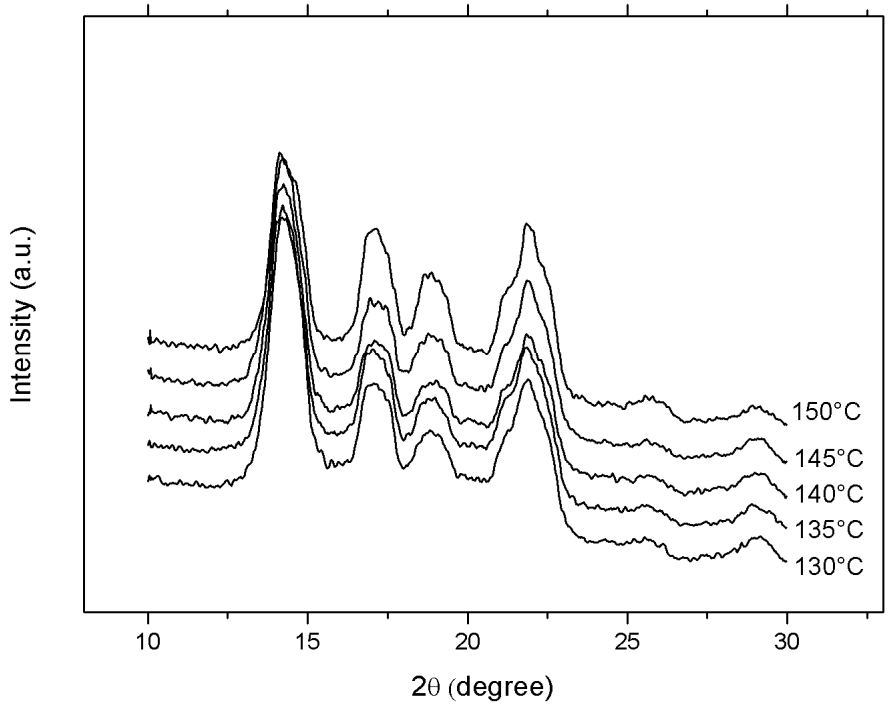

Fig. 32: WAXS patterns of LCB PP isothermally crystallized at different crystallization temperatures

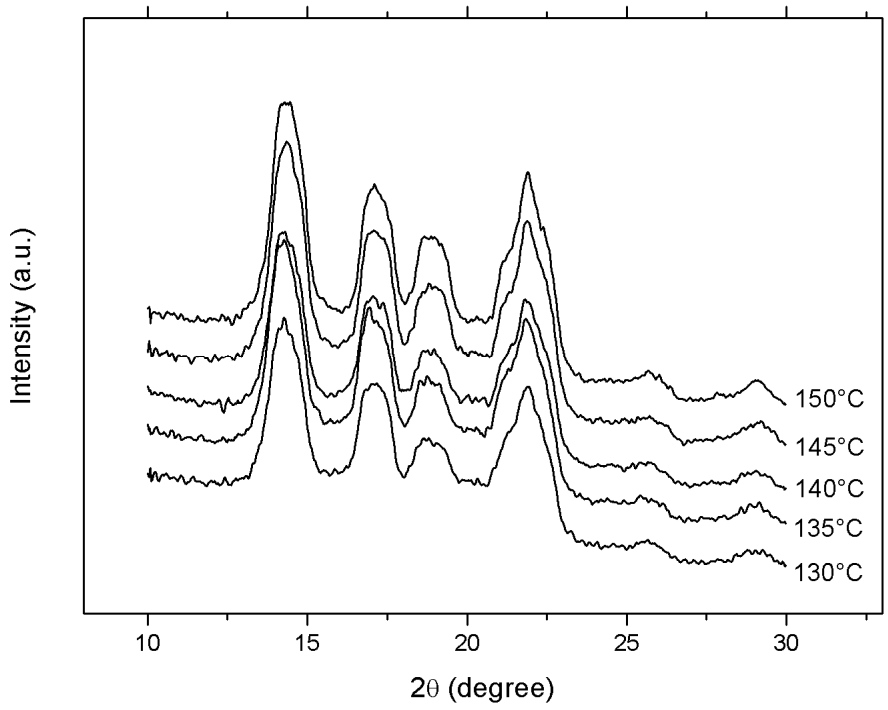

Fig. 33: WAXS patterns of LCB PP+NA isothermally crystallized at different crystallization temperatures

8.3 Polarized light microscopy

The morphology formed during isothermal crystallization of the samples was observed via polarized light microscopy and corresponding micrographs are shown in *Figs. 34* and *35*. It can be seen that linear PP shows relatively large spherulites with distinct boundaries and their size further increases with increasing crystallization temperature. Such structure was formed via homogeneous nucleation. On the other hand, in LCB PP and LCB PP+NA no spherulites are observed. It is presumed that they are very small, not observable via polarized light microscopy. Such structure was initiated by heterogeneous nucleation. In *Fig. 35* the grainy structure is evident in LCB PP and LCB PP+NA, however each crystallites are not distinguished. For better structure analysis scanning electron microscopy should be used. Nevertheless, it is evident that the structure formed in LCB PP and LCB PP+NA is quite similar and according the results does not significantly changes with increasing T_c.

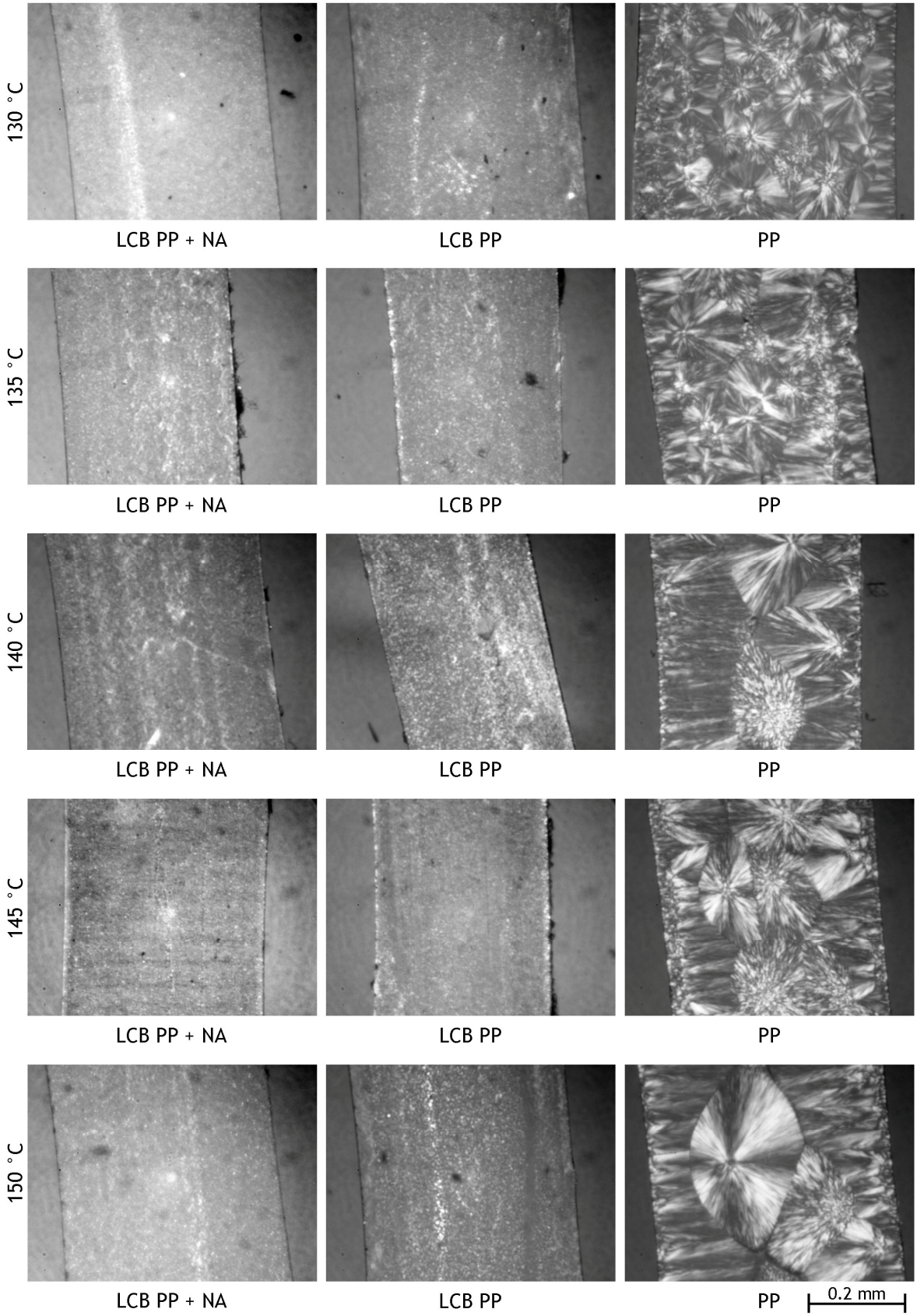

Fig. 34: Micrographs of isothermally crystallized samples, low magnitude

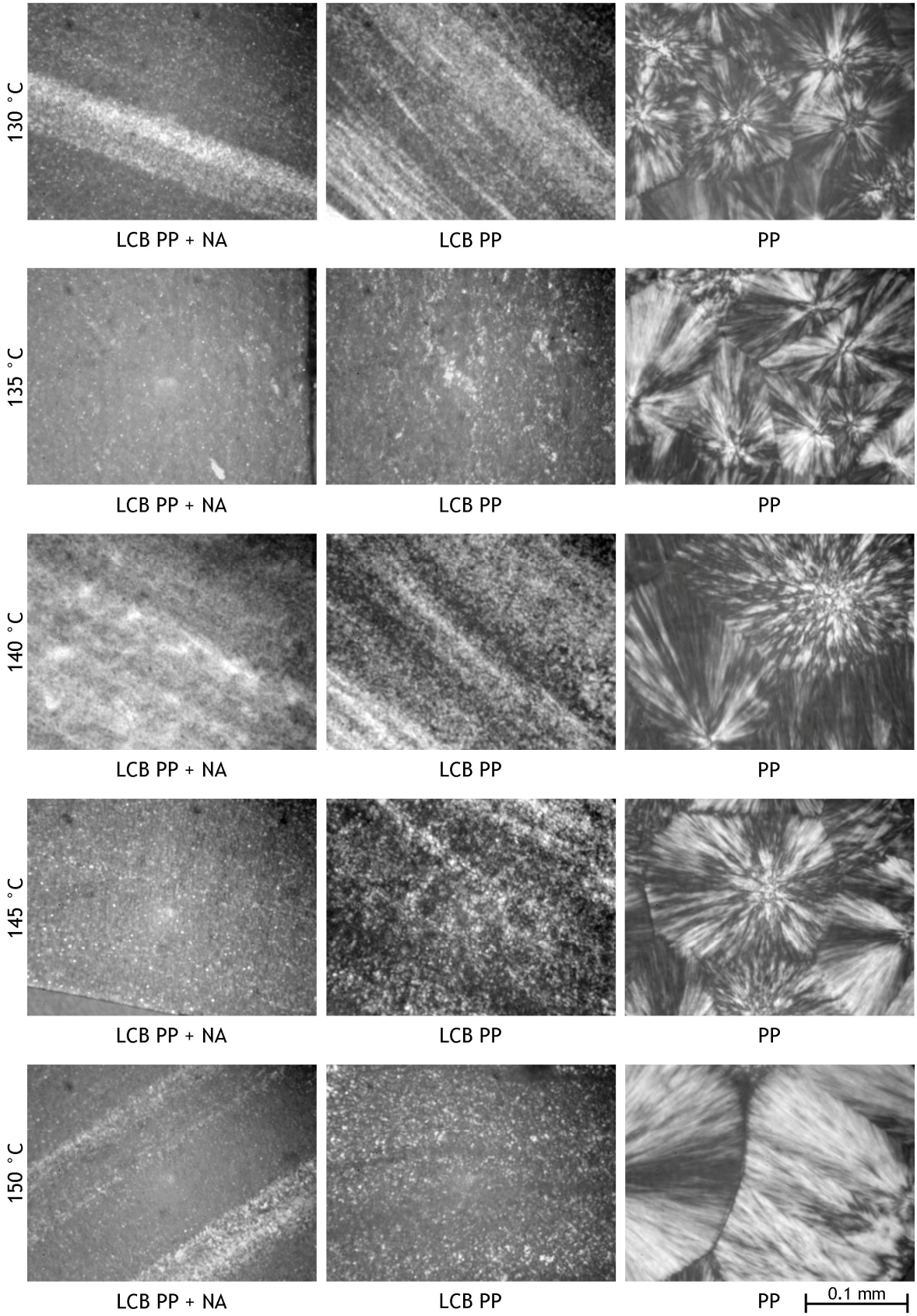

Fig. 35: Micrographs of isothermally crystallized samples, high magnitude

IV. CONCLUSION

In this master thesis the presence of common α-nucleating/clarifying agent Millad 3988 on both isothermal and non-isothermal crystallization and morphology of long chain branched polypropylene was examined. For comparison, linear polypropylene was studied as well. For these purposes, differential scanning calorimetry, wide-angle X-ray scattering and polarized light microscopy were employed. Optical properties were also analyzed.

Optical properties are often decisive for packaging technologies where LCB PP is often used. The results showed that linear PP possessed the highest haze as was expected. On the other hand, LCB PP showed the lowest haze which was most probably caused by long chain branches that played a role of nucleating/clarifying agent. The addition of Millad 3988 into LCB PP did not lead to decrease of haze, contrary it significantly increased the haze as compared to neat LCB PP.

Non-isothermal crystallization analysis showed that LCB PP crystallized at higher temperature as compared to linear PP (112.9 vs. 128.8 °C). This proved the preposition that long chain branches caused the heterogeneous nucleation. The addition of Millad 3988 led to further increase of crystallization temperature to the value of 130.8 °C. Linear PP possessed the highest melting temperature from all non-isothermally crystallized samples. The melting temperatures of both other materials (LCB PP and LCB PP+NA) were similar. The crystallinity of non-isothermally crystallized samples was the highest at linear PP and the lowest at LCB PP. The addition of clarifying agent caused the increase of crystallinity over 8 %. Only α-phase was detected in all the materials.

Isothermal crystallization was performed at several temperatures. It was found that LCB PP and LCB PP+NA crystallized significantly faster that linear PP. The halftime of crystallization of linear PP was 55.4 min while that of LCB PP and LCB PP+NA was 7.6 and 5.6 min, respectively. The values of melting temperature of LCB PP and LCB PP+NA were similar while that of linear PP were somewhat higher. In all cases of materials the crystallinity increased with increasing crystallization temperature. No β-phase presence in the structure of all materials was observed.

Polarized light microscopy evaluation revealed that linear PP consisted of large spherulites and their size further increase with increasing crystallization temperature in the case of isothermal crystallization. The structure formed in LCB PP and LCB PP+NA was very fine and each crystallites were not observable using light microscopy. Moreover, the

structure did not change with increasing crystallization temperature in the case of isothermal crystallization.

In this work it was revealed that the addition of Millad 3988 a-nucleating/clarifying agent into the long chain branched polypropylene did not lead to increase of clarity of the material and moreover it did not significantly influence the crystallization.

BIBLIOGRAPHY

[1] http://www.bpf.co.uk/Plastipedia/Polymers/PP.aspx (8.5.2010)

[2] Weng, W. et al.: Macromolecules, 2002, vol. 35, p. 3838

[3] Jinghua, T., Wei, Y., Chixing, Z.: J. Appl. Polym. Sci., 2007, vol. 104, p. 3592

[4] Graebling, D.: Macromolecules, 2002, vol. 35, p. 4602

[5] Liu, Z. L.; Meng, B.; Tian, W. D.: Mod. Plast. Process. Appl., 2002, vol. 14, p. 17

[6] Marco, C., Ellis, G., Gomez, M. A., Arribas, J. M.: J. Appl. Polym. Sci., 2002, vol. 84, p. 2440

[7] Shepard, T.A. et al.: J. Polym. Sci. Polym. Phys., 1997, vol. 35, p. 2617

[8] Kristiansen, M. et al.: Macromolecules, 2003, vol. 36, p. 5150

[9] Výchopňová, J., Čermák, R., Obadal, M., Raab, M., Verney, V., Commereuc, S.: Polym. Degrad. Stabil., 2007, vol. 92, p. 1763

[10] Šenkyřík, J., Master thesis, 2007, Tomas Bata University in Zlin, Faculty of technology

[11] Borsig, E. et al.: Eur. Polym. J., 2008, vol. 44, p. 200

[12] http://www.lsp.uni-erlangen.de/english/projects/auhl/auhl.html (10.4.2010)

[13] Oliver et al.: Patent Application Publication, pub. No.: US 2006/0167128 A1

[14] Ratzsch et al.: Prog. Polym. Sci., 2002, vol. 27, p. 1195

[15] http://www.dtic.mil/cgi-bin/GetTRDoc?Location=U2&doc=GetTRDoc.pdf&AD=ADA486409 (16.4.2010)

[16] Lagendijk R. P. et al.: Polymer, 2001, vol. 42, p. 10035

[17] http://www.thefreelibrary.com/Rheological+properties+of+blends+of+linear+and+long-chain+branched-a0216990551 (13.4.2010)

[18] Sugimoto, M. et al.: Rheol. Acta, 2006, vol. 46, p. 33

[19] Borealis promotional material: Daploy HMS Polypropylene for Foam Extrusion

[20] http://www.freshpatents.com/-dt20090618ptan20090156743.php (11.3.2010)

[21] http://www.hyperformnucleatingagents.com/SiteCollectionDocuments/Hyperform/Documents/Nucleating%20Agents%20PP.pdf (25.2.2010)

[22] Hoffmann, K., Huber, G., Mader, D.: Macromol. Symp., 2001, vol. 176, p. 83

[23] http://www.cliffsnotes.com/WileyCDA/CliffsReviewTopic/Gibbs-Free-Energy.topicArticleId-21729,articleId-21724.html (22.4.2010)

[24] Varga J., Crystallization, Melting and Supermolecular Structure of Isotactic Polypropylene. In: Karger-Kocsis J. Polypropylene: Structure, Blends and Composites, vol. 3, Chapman and Hall, London, 1995, ISBN: 0 412 58430 0

[25] http://trends.ellerdale.com/topics/view/008c-725f/Avrami+equation.html (22.4.2010)

[26] http://www.iupac.org/goldbook/A00545.pdf (22.4.2010)

[27] Maier, C., Calafut, T.: Polypropylene: The Definitive User´s Guide and Databook, William Andrew Inc., 1998, ISBN 1884207588

[28] Varga, J.: J. Macromol. Sci. Phys., 2002, vol. 41, p. 1121

[29] Raab, M., Kotek, J., Baldrian, J., Grellmann, W.: J. Appl. Polym. Sci., 1998, vol. 69, p. 2255

[30] Kotek, J., Raab, M., Baldrian, J., Grellmann, W.: J. Appl. Polym. Sci., 2002, vol. 85, p. 1174

[31] http://composite.about.com/library/glossary/n/bldef-n3664.htm (25.2.2010)

[32] Zweifel, H.: Plastics Additives Handbook, Munich: Hanser, 2001, ISBN 1-56990-295-X

[33] Kristiansen, M. et al.: Macromolecules, 2003, vol. 36, p. 5150

[34] Ferrage, E. et al.: J. Mat. Sci., 2002, vol. 37, p. 1561

[35] Shanks, R. A., Tiganis, B. E., Nucleating Agents for Thermoplastics. In: Pritchard, G., Plastics Additives – An A-Z References, Springer-Verlag, 1998, ISBN 978-1-59124-134-8

[36] http://www.specialchem4polymers.com/tc/polyolefin-nucleators/index.aspx (5.3.2010)

[37] Libster, D., Aserin, A., Garti, N.: Polym. Adv. Technol., 2007, vol. 18, p. 685

[38] http://www.nicnas.gov.au/publications/CAR/new/NA/NAFULLR/NA0100FR/NA179FR.pdf (15.2.2010)

[39] http://www.mayzo.com/pdf/PP-Geogrid-Presentation.pdf (12.3.2010)

[40] http://www.freepatentsonline.com/20100010168.pdf (15.3.2010)

[41] Marco, C., Gomez, M. A., Ellias, G., Arribas, J. M.: J. Appl. Polym. Sci., 2002, vol. 84, p. 1669

[42] Lugão A. B. et al.: IPEN – Progress Report 2002–2004, Chemical and Environmental Technology Center

[43] Hoffmann, J. D., Weeks, J. J.: J. Chem. Phys., 1962, vol. 37, p. 1723

[44] Tian, J., Wei Y., Chixing Z.: J. Appl. Polym. Sci., 2007, vol. 104, p. 3592

[45] Zeng, W., Wang, J.,Feng, Z., Dong, J., Yan, S.: Colloid Polym. Sci., 2005, vol. 284, p. 322

[46] Agarwal, P. K.; Somani, R. H.; Weng, W. Q.; Mehta, A.: Macromolecules, 2003, vol. 36, p. 5226

LIST OF ABBREVIATIONS

LCB PP	long chain branched polypropylene
PP	polypropylene
iPP	isotactic polypropylene
PE	polyethylene
PVC	polyvinyl chloride
LCB	long chain branching
e.g.	exempli gratia
NA	nucleating agent
DVB	divinylbenzene
FS	furfuryl sulphide
i.e.	id est
PODIC	peroxydicarbonate
SCB	short chain branching
DBS	1,2,3,4-bis-dibenzylidene sorbitol
DOS	1,2,3,4-bis-(p-methoxybenzylidene sorbitol)
MBDS	1,2,3,4-bis-(p-methylbenzylidene sorbitol)
DMDBS	1,3;2,4-di-(3,4-dimethylbenzylidene sorbitol)
wt.%	weight percentage
Fig.	figure
WAXS	wide-angle X-ray scattering
PLM	polarized light microscopy
DSC	differential scanning calorimetry
approx.	approximate

LIST OF FIGURES

LIST OF TABLES

LIST OF EQUATIONS